(2-methylphenanthrene)- and (3-methylphenanthrene)-chromium tricarbonyl isomers suggests that this isomer could be $Cr(CO)_3(\eta^6\text{-}4\text{-}CH_3C_{14}H_9)$. The splitting pattern is correct for this assignment. Finally, the literature reports the methyl resonance of this compound to be observed at 2.67 ppm in $CDCl_3$.[9] A fourth resonance is observed in the methyl region at δ 2.54 for most of the reaction mixtures. The compound responsible is present in low concentration, never more than 5% of the products, and is tentatively assumed to be $Cr(CO)_3(\eta\text{-}1\text{-}CH_3C_{14}H_9)$. The low concentration of this species precludes assignment or location of the other resonances for this isomer. Steric constraints could be the major reason for the observation of its low concentration.

In other instances the effects of varying temperature and time were less significant. Lithiation of $Cr(CO)_3(\eta^6\text{-}5\text{-}CH_3OC_{10}H_7)$ at -95 °C followed by warming to -42 °C and addition methyl iodide gave the same products, $Cr(CO)_3(\eta^6\text{-}2\text{-}CH_3\text{-}5\text{-}CH_3OC_{10}H_6)$ and $Cr(CO)_3(\eta^6\text{-}3\text{-}CH_3\text{-}5\text{-}CH_3OC_{10}H_6)$, in 25% yield with the amount of the former slightly increased (ratio of 35:65 instead of 26:74). Similarly the ratio of $Cr(CO)_3(\eta^6\text{-}2,6\text{-}(CH_3O)_2\text{-}3\text{-}CH_3C_{10}H_5)$ to $Cr(CO)_3(\eta^6\text{-}2,6\text{-}(CH_3O)_2\text{-}1\text{-}CH_3C_{10}H_5)$ was seen to vary in an insignificant manner. At -95 °C an 81:19 ratio was measured whereas at -42 °C the ratio was 86:14. In neither of these instances was an additional isomer detected.

Ligand Bridging and Chelation of Tetracobalt Clusters with Difunctional Phosphines

M. G. Richmond and J. K. Kochi*

Department of Chemistry, University of Houston, University Park, Houston, Texas 77004

The interaction of the tetracobalt carbonyl cluster $Co_4(CO)_{10}(\mu_4\text{-}PPh)_2$ (I) with various bidentate phosphines such as $Ph_2P(CH_2)_nPPh_2$ was examined under both thermal conditions at >80 °C and electron-transfer chain (ETC) catalysis at 25 °C. With diphosphines possessing short carbon backbones (n = 1 and 2), the disubstituted clusters $Co_4(CO)_8(PPh)_2(P \frown P)$(III) were isolated in high yields under electron-transfer chain catalysis and shown to be the same as those derived in low yields from the thermal reaction. Structure elucidation by X-ray crystallography has established two modes of ligand binding to the tetracobalt cluster, in which the diphosphine either bridged a pair of adjacent cobalt atoms or chelated a single cobalt atom. The dynamic properties of such bridged and chelated clusters in solution were deduced from the temperature-dependent ^{31}P and ^{13}C NMR spectra of the diphosphine and carbonyl (terminal and bridging) ligands, respectively. The higher diphosphine homologues with n = 3 and 4 afforded mono- and disubstituted clusters, the relative amounts of which depended on whether the substitutions were carried out by ETC stimulation or under thermal conditions.

Introduction

Polydentate phosphines can control the stereochemistry and influence the lability of ligands in organometallic complexes.[1–6] The effects of polydentate phosphines in altering the product distributions in catalytic processes are also well-documented.[3,7] Relevant to the latter, poly-dentate phosphines have been shown to maintain the metal clusters intact under a variety of conditions in which the unsubstituted cluster undergoes fragmentation. For example, the triruthenium cluster capped with a tripod silaphosphine ligand $Ru_3(CO)_9[Si(Me)(PBu_2)_3]$ has been shown to be resistant to fragmentation under the conditions of the Fischer–Tropsch reactions.[8] Furthermore the tetranuclear relatives $M_4(CO)_9[HC(PPh_2)_3]$ where M = Co, Rh, and Ir are stable at high CO pressures.[9] By way of comparison, the parent carbonyl clusters are readily cleaved to species of lower nuclearity upon exposure to carbon monoxide as well as to H_2/CO mixtures.[10]

(1) Collman, J. P.; Hegedus, L. S. *Principles and Applications of Organotransition Metal Chemistry*; University Science Books: Mill Valley, Ca, 1980.

(2) McAuliffe, C. A.; Levason, W. *"Phosphine, Arsine and Stilbine Complexes of the Transition Elements*; Elsevier: New York, 1979.

(3) For the use of polydentate phosphines in catalysis, see: (a) *Adv. Chem. Ser.* **1982**, *No. 196* and references within. (b) Pignolet, L. H., Ed. *Homogeneous Catalysis with Metal Phosphine Complexes*; Plenum: New York, 1983. (c) Valentine, D. S., Jr.; Scott, J. W. *Synthesis* **1976**, 329. (d) Kagan, H. B. *Pure Appl. Chem.* **1975**, *43*, 401. (e) Halpern, J.; Riley, D. P.; Chan, A. S. C.; Pluth, J. J. *J. Am. Chem. Soc.* **1977**, *99*, 8055. (f) Chan, A. S. C.; Halpern, J. *J. Am. Chem. Soc.* **1980**, *102*, 838.

(4) (a) King, R. B. *Acc. Chem. Res.* **1972**, *5*, 177. (b) *Acc. Chem. Res.* **1980**, *13*, 243.

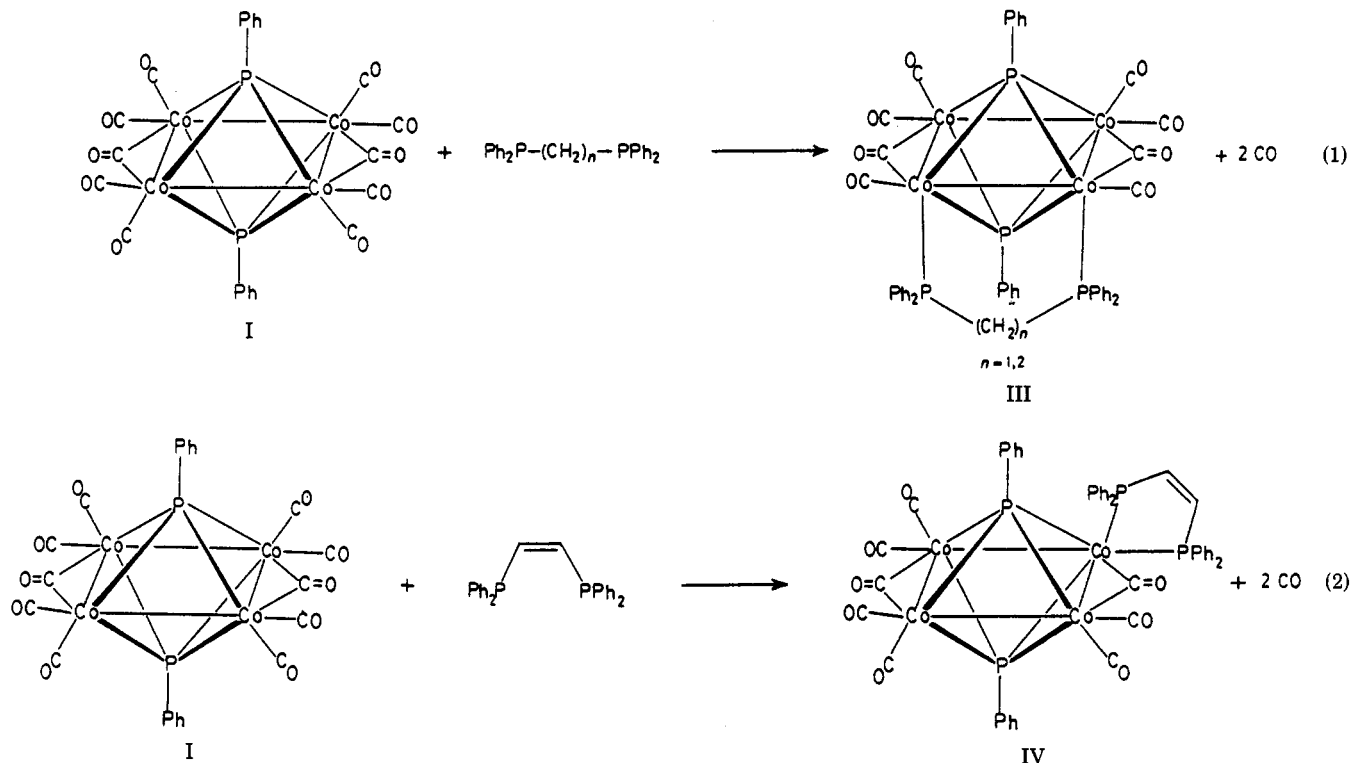(5) Mason, R.; Meek, D. W. *Angew. Chem., Int. Ed. Engl.* **1978**, *18*, 183.

(6) (a) Murata, K.; Matsuda, A. *Bull. Chem. Soc. Jpn.* **1980**, *33*, 214. (b) *Nippon Kagaku Kaishi* **1981**, *8*, 1335. (c) *Kagaku Gijutsu Kenkyusho Hokoku* **1984**, *79*, 155.
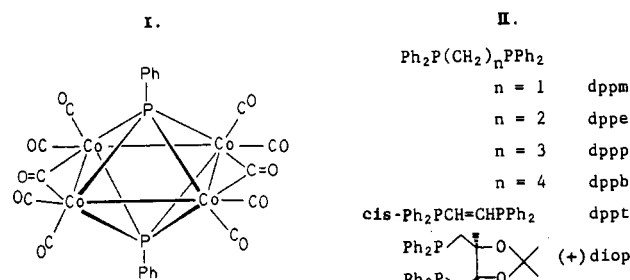
(7) (a) Pittman, C. U.; Wilemon, G. M.; Wilson, D. W.; Ryan, R. C. *Angew. Chem., Int. Ed. Engl.* **1980**, *19*, 478. (b) Pittman, C. U.; Richmond, M. G.; Wilemon, G. M.; Absi-Halabi, M. In *Catalysis of Organic Reactions*, Kosak, J. R., Ed.; Marcel Dekker: New York, 1984; Chapter 5.

(8) (a) de Boer, J. J.; van Doorn, J. A.; Masters, C. *J. Chem. Soc., Chem. Commun.* **1978**, 1005. (b) Masters, C. *Adv. Organomet. Chem.* **1979**, *17*, 61.

(9) (a) Arduini, A. A.; Bahsoun, A. A.; Osborn, J. A.; Voelker, C. *Angew. Chem., Int. Ed. Engl.* **1980**, *19*, 1024. (b) Bahsoun, A. A.; Osborn, J. A.; Voelker, C.; Bonnet, J. J.; Lavigne, G. *Organometallics* **1982**, *1*, 1114.

$$I + Ph_2P-(CH_2)_n-PPh_2 \longrightarrow III + 2\ CO \quad (1)$$

$$n = 1, 2$$

$$I + Ph_2P-CH=CH-PPh_2 \longrightarrow IV + 2\ CO \quad (2)$$

We feel that the stabilization of metal clusters could also be achieved with bidentate phosphines. Such intact clusters may then serve as homogeneous counterparts to heterogeneous catalysts.[11] Particularly noteworthy is the observation that the presence of these ligands during hydroformylation with a tetracobalt catalyst leads to higher ratios of linear to branched aldehydes.[7] Since the fate of the phosphine ligands in this catalytic system is unknown, we examined the interaction of the tetracobalt cluster I with a homologous series of bidentate phosphines II of varying chain lengths, as shown. The principal objectives

I.	II.	
	$Ph_2P(CH_2)_nPPh_2$	
	n = 1	dppm
	n = 2	dppe
	n = 3	dppp
	n = 4	dppb
	cis-$Ph_2PCH=CHPPh_2$	dppt
	$Ph_2P \diagup \diagdown O \diagdown$	(+)diop

of this study are the identification and structural characterization of the cluster products, particularly with regard to the binding of the various diphosphine ligands II to the tetracobalt core of I.

Results

I. Thermal Reactions of the Tetracobalt Cluster I with Bidentate Phosphines. When a red solution of the tetracobalt cluster $Co_4(CO)_{10}(\mu_4\text{-}PPh)_2$ (I) in either benzene or toluene was exposed to the diphosphine dppm at 50–80 °C, 2 mol of CO was liberated and the disubstituted cluster $Co_4(CO)_8(PPh)_2(dppm)$ (IIIa) was isolated. The analogues dppe and dppt yielded similar products IIIb and IV, respectively. In each case the replacement of a pair of carbonyl ligands was consistent with the elemental analyses of the pure products IIIa,b and IV, which were successfully isolated as purple-black single crystals (see Experimental Section). The use of more forcing conditions (>80 °C for longer periods) to promote further substitution led to extensive cluster degradation as well as intermolecular ligation of a pair of tetracobalt clusters via the bifunctional ligands.

The structural similarity of the substitution products IIIa and IIIb was shown by the comparison of the carbonyl region of the IR spectra in Figure 1. The shift (~35 cm^{-1}) of the bridging carbonyl band from 1870 cm^{-1} in the parent I was particularly diagnostic of disubstitution in the tetracobalt cluster.[12] Moreover the appearance of this band as a single absorption was indicative of the two bridging carbonyls that exist in equivalent environments. We thus concluded that disubstitution of I by dppm and dppe must have occurred across the non-carbonyl-bridged Co(1)–Co(4) bond to yield the symmetric structure shown in eq 1. The appearance of a shoulder at ~1990 cm^{-1} of the terminal carbonyl band of $Co_4(CO)_8(PPh)_2(dppe)$, which is absent in the dppm analogue, suggested the existence of additional conformational effects in IIIb which are associated with the more flexible dppe ligand. By contrast, the structure of the dppt analogue IV differed from that of either IIIa or IIIb. Thus the appearance of two bridging carbonyl bands at 1849 and 1813 cm^{-1} in the IR spectrum in Figure

(10) (a) Chini, P.; Heaton, B. *Top. Curr. Chem.* **1977**, *71*, 53. (b) Dombek, B. D. *J. Am. Chem. Soc.* **1980**, *102*, 6855. (c) Bor, G.; Dietler, U. K. Pino, P.; Poe, A. *J. Organomet. Chem.* **1978**, *154*, 301. (d) Vidal, J. L.; Walker, W. E. *Inorg. Chem.* **1981**, *20*, 249. (e) Whyman, R. *J. Chem. Soc., Dalton Trans.* **1972**, 1375. (f) Whyman, R. *J. Chem. Soc., Dalton Trans.* **1972**, 2294.

(11) For discussions of polynuclear clusters as homogeneous examples of heterogeneous catalysts and the cluster-surface analogy, see: (a) Muetterties, E. L.; Rhodin, T. N.; Band, E.; Brucker, C. F.; Pretzer, W. R. *Chem. Rev.* **1979**, *79*, 91. (b) Muetterties, E. L. *Science (Washington, D.C.)* **1977**, *196*, 839. (c) Muetterties, E. L.; Krause, M. J. *Angew. Chem., Int. Ed. Engl.* **1983**, *22*, 135. (d) Muetterties, E. L. *Bull. Soc. Chim. Belg.* **1975**, *84*, 959; **1976**, *85*, 451. (e) Pittman, C. U.; Ryan, R. C. *Chemtech.* **1978**, 170. (f) Smith, A. K.; Basset, J. M. *J. Mol. Catal.* **1977**, *2*, 229. (g) Muetterties, E. L. *J. Organomet. Chem.* **1980**, *200*, 177. (h) Muetterties, E. L. *Pure Appl. Chem.* **1982**, *54*, 83.

(12) (a) Cotton, F. A.; Wilkinson, G. *Advanced Inorganic Chemistry*, 3rd Ed.; Wiley: New York, 1972; Chapter 22. (b) Purcell, K. F.; Kotz, J. C. *Inorganic Chemistry*; W. B. Saunders: Philadelphia, 1977; Chapter 18. (c) Cotton, F. A.; Kraihanzel, C. S. *J. Am. Chem. Soc.* **1962**, *84*, 4432.
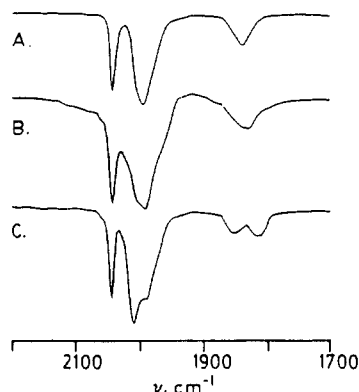
Figure 1. Infrared spectra of the carbonyl region for (A) Co_4-$(CO)_8(PPh)_2(dppm)$ (IIIa), (B) $Co_4(CO)_8(PPh)_2(dppe)$ (IIIb), and (C) $Co_4(CO)_8(PPh)_2(dppt)$ (IV) in dichloromethane at 25 °C.

1c was not consistent with a bridging phosphine ligand as in IIIa and IIIb. However, disubstitution on a single cobalt atom (i.e., in a chelating mode) would have rendered the pair of bridging carbonyls sufficiently different as to appear as two separate absorption bands. If so, the band at lower energy (1813 cm^{-1}) can be assigned to the bridging carbonyl that is flanked by the chelating diphosphine.[12] Indeed the bridging and chelating nature of bidentate phosphines as described in eq 1 and 2 for IIIa,b and IV, respectively, was established by X-ray crystallography (vide infra).

The thermal reactions of the tetracobalt cluster I with the higher diphosphines dppp and dppb with n = 3 and 4 were also carried out at 50–80 °C in toluene. The disubstituted derivatives $Co_4(CO)_8(PPh)_2(dppp)$ and Co_4-$(CO)_8(PPh_2)(dppb)$ were isolated in 5–20% yields, but the spectral analysis indicated that these products were formed as mixtures containing bridging and chelating diphosphine ligands.[13] Moreover a large amount of unidentified material was obtained that was either insoluble or unstable to chromatographic adsorbents.[14]

II. Electron-Transfer Chain Catalysis of Diphosphines with the Tetracobalt Cluster I.

Carbon monoxide was spontaneously liberated at room temperature when a catalytic amount (~1 mol %) of potassiobenzophenone was simply added to a THF solution of the tetracobalt cluster I and dppm. Workup of the reaction mixture yielded 60% of the disubstitution product IIIa which was identical with that obtained in eq 1. The utilization of benzophenone ketyl to effect electron-transfer chain (ETC) catalysis of the facile and selective ligand substitution in polynuclear clusters is well-established.[16–18]
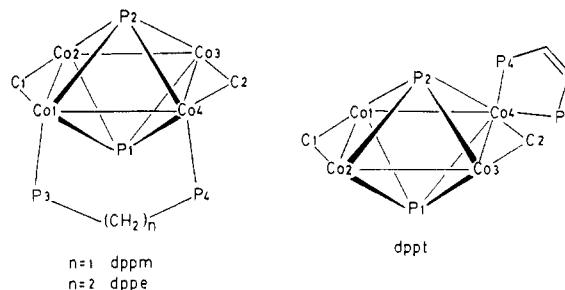
Table I. Selected Bond Lengths (Å) in the Disubstituted Tetracobalt Clusters IIIa,b and IV[a]

	dppm	dppe	dppt
Co(1)–Co(2)	2.538 (2)	2.525 (2)	2.513 (3)
Co(1)–Co(4)	2.673 (2)	2.688 (2)	2.878 (3)
Co(2)–Co(3)	2.710 (2)	2.688 (2)	2.645 (3)
Co(3)–Co(4)	2.521 (2)	2.534 (2)	2.534 (3)
Co(1)–C(1)	1.855 (15)	1.915 (12)	1.946 (15)
Co(2)–C(1)	1.984 (14)	1.984 (13)	1.868 (14)
Co(3)–C(2)	2.040 (12)	2.067 (11)	1.998 (14)
Co(4)–C(2)	1.912 (12)	1.840 (12)	1.907 (15)
P(1)···P(2)	2.546 (4)	2.548 (3)	2.509 (5)

[a] The number in the parentheses is the estimated standard deviation in the least significant digit.

Table II. Selected Bond Angles (deg) in the Diphospine-Substituted Tetracobalt Clusters IIIa,b and IV[a]

	dppm	dppe	dppt
Co(2)–Co(1)–Co(4)	90.25 (6)	90.38 (6)	87.8 (1)
Co(1)–Co(2)–Co(3)	89.37 (6)	89.82 (6)	92.6 (1)
Co(2)–Co(3)–Co(4)	89.78 (6)	90.19 (6)	92.7 (1)
Co(1)–Co(4)–Co(3)	90.60 (6)	89.62 (6)	86.87 (9)
Co(1)–P(1)–Co(2)	68.50 (9)	68.90 (9)	67.7 (1)
Co(1)–P(1)–Co(4)	72.64 (9)	73.6 (1)	80.7 (2)
Co(1)–P(2)–Co(2)	69.2 (1)	68.61 (9)	67.1 (1)
Co(1)–P(2)–Co(4)	73.34 (9)	73.87 (9)	111.1 (2)
Co(1)–C(1)–Co(2)	82.7 (6)	80.7 (6)	82.4 (6)
Co(3)–C(2)–Co(4)	79.2 (5)	80.7 (5)	80.9 (6)
Co(4)–Co(1)–P(3)	93.07 (8)	111.19 (9)	
Co(1)–Co(4)–P(4)	98.78 (9)	99.61 (9)	118.0 (2)

[a] Numbers in parentheses are estimated standard deviations in the least significant digit. Numbering scheme as in Table I.

Indeed we showed earlier that the substitution of I with monophosphines occurred by a dissociative loss of carbon monoxide under ETC catalytic conditions.[19] What is unusual in this study is the substitution of a *pair* of carbonyl ligands under conditions in which monophosphines merely undergo reaction at a single ligand site.[19] Steric factors undoubtedly contribute to disubstitution since the

(13) (a) The chelating nature of the disubstituted clusters $Co_4(CO)_8$-$(PP)(PPh)_2$ is suggested by the presence of two bridging carbonyl bands in the IR spectrum. By contrast, the bridging isomer gives only one bridging carbonyl band. (b) For a recent discussion illustrating the differences in IR spectral properties of bridging and chelating diphosphines in osmium clusters, see: Deeming, A. J.; Donovan-Mtunzi, S.; Kabir, S. E. *J. Organomet. Chem.* **1984**, *276*, C65.

(14) It is possible that the initially coordinated phosphine underwent further transformations on the clusters. For example, oxidative cleavage and cyclometalation of phosphines are known to occur in a variety of clusters that possess bridging and chelating diphosphine ligands.[15]

(15) (a) Lavigne, G.; Bonnet, J. J. *Inorg. Chem.* **1981**, *20*, 2713. (b) Lavigne, G.; Lugan, N.; Bonnet, J. J. *Organometallics* **1982**, *1*, 1040. (c) Harding, M. M.; Nicholls, B. S.; Smith, A. K. *J. Chem. Soc., Dalton Trans.* **1983**, 1479. (d) Clucas, J. A.; Foster, D. F. Harding, M. M.; Smith, A. K. *J. Chem. Soc., Chem. Commun.* **1984**, 949. (e) Ibid. *J. Chem. Soc., Chem. Commun.* **1985**, 1280. (f) Albano, V. G.; Braga, D.; Ros, R.; Scrivanti, A. *J. Chem. Soc., Chem. Commun.* **1985**, 866.

(16) For a general discussion of the ETC reaction and catalytic implications, see: (a) Chanon, M.; Tobe, M. L. *Angew. Chem., Int. Ed. Engl.* **1982**, *21*, 1. (b) Bunnett, J. F. *Acc. Chem. Res.* **1978**, *11*, 413. (c) Saveant, J. M. *Acc. Chem. Res.* **1980**, *13*, 323. (d) Miholova, D.; Vlcek, A. A. *J. Organomet. Chem.* **1982**, *240*, 413.

(17) For substitution reactions proceeding by ETC catalysis, see: (a) Arewgoda, C. M.; Robinson, B. H.; Simpson, J. *J. Am. Chem. Soc.* **1983**, *105*, 1893. (b) Bezems, G. J.; Rieger, P. H.; Visco, S. *J. J. Chem. Soc., Chem. Commun.* **1981**, 265. (c) Arewgoda, C. M.; Rieger, P. H.; Robinson, B. H.; Simpson, J.; Visco S. *J. Am. Chem. Soc.* **1982**, *104*, 5633. (d) Arewgoda, C. M.; Robinson, B. H.; Simpson, J. *J. Chem. Soc., Chem. Commun.* **1982**, 283. (e) Jensen, S.; Robinson, B. H.; Simpson, J. *J. Chem. Soc., Chem. Commun.* **1983**, 1081. (f) Bruce, M. I.; Hambley, T. W.; Nicholson, B. K.; Snow, M. R. *J. Organomet. Chem.* **1982**, *235*, 83. (g) Bruce, M. I.; Kehoe, D. C.; Matisons, J. G.; Nicholson, B. K.; Rieger, P. H.; Williams, M. L. *J. Chem. Soc., Chem. Commun.* **1982**, 442. (h) Downard, A. J.; Robinson, B. H.; Simpson, J. *Organometallics* **1986**, *5*, 1122; **1986**, *5*, 1132; **1986**, *5*, 1140.

(18) Other examples of ETC catalytic reactions involving mononuclear organometallic compounds include: (a) Hershberger, J. W.; Klingler, R. J.; Kochi, J. K. *J. Am. Chem. Soc.* **1982**, *104*, 3034; **1983**, *105*, 61. (b) Hershberger, J. W.; Amatore, C.; Kochi, J. K. *J. Organomet. Chem.* **1983**, *250*, 345. (c) Zizelman, P. M.; Amatore, C.; Kochi, J. K. *J. Am. Chem. Soc.* **1984**, *106*, 3771. (d) Darchen, A. *J. Chem. Soc., Chem. Commun.* **1983**, 768. (e) Connelly, N. G.; Geiger, W. E. *Adv. Organomet. Chem.* **1984**, *23*, 1 and references within.

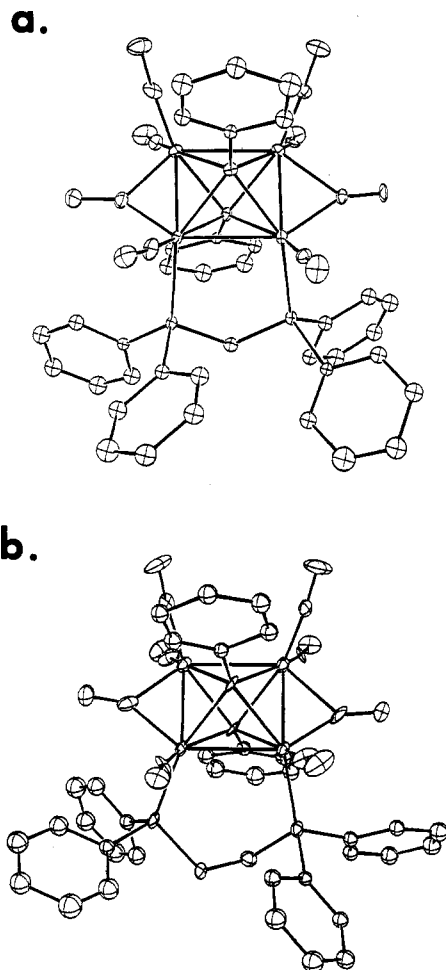(19) Richmond, M. G.; Kochi, J. K. *Inorg. Chem.* **1986**, *25*, 656.

a.

b.

Figure 2. ORTEP diagrams of (a) $Co_4(CO)_8(\mu_4\text{-PPh})_2(dppm)$ (IIIa) and (b) $Co_4(CO)_8(\mu_4\text{-PPh})_2(dppe)$ (IIIb) showing the bridging of the Co(1)–Co(4) bond by the diphosphine. For clarity the solvent (CH_2Cl_2) and the hydrogens are omitted.

Figure 3. ORTEP diagram of $Co_4(CO)_8(\mu_4\text{-PPh})_2(dppt)$ (IV) showing the chelation of the diphosphine to Co(4). Hydrogens are omitted for clarity.

Figure 4. The $^{31}P\{^1H\}$ NMR spectra of (A) $Co_4(CO)_8(PPh)_2$-(dppm), (B) $Co_4(CO)_8(PPh)_2(dppe)$, and (C) $Co_4(CO)_8(PPh)_2(dppt)$ in dichloromethane solution at 198 K.

other diphosphines dppe and dppt afforded the corresponding disubstituted clusters IIIb and IV in good yields when treated with I and catalytic amounts of potassiobenzophenone. In each case the products were the same as those obtained in the much less efficient thermal process.

Carbon monoxide was also readily liberated when the higher diphosphine homologues dppp and dppb with n = 3 and 4 were subjected to ETC catalysis of the tetracobalt cluster I. However, inspection of the IR spectra of the products indicated that only monosubstitution occurred since they were all identical with the spectrum of the known[20] monosubstituted $Co_4(CO)_9(PPh_2)(PPh_3)$ in the carbonyl stretching region from 1700 to 2100 cm^{-1}. Furthermore the uncoordinated, dangling phosphine moiety in these clusters was readily observed as a singlet resonance at high field ($\delta \sim -20$) in the ^{31}P NMR spectra.[21] The optically active diop ligand (n = 4 but which is somewhat constrained) also afforded only the monosubstitution product under ETC catalysis.

The divergent behavior of the homologous diphosphines $Ph_2P(CH_2)_nPPh_2$ thus underscored the high selectivity that can be achieved in ligand substitution of polynuclear clusters under ETC catalysis.

III. Molecular Structures of the Disubstituted Tetracobalt Clusters.

The dispositions of the diphosphine ligands in the cluster polyhedron were established by X-ray crystallography of the disubstituted products derived from dppm, dppe, and dppt. The ORTEP diagrams in Figure 2 established the bridging nature of the dppm and dppe ligands in IIIa and IIIb, respectively. As earlier deduced from the IR spectra (vide supra), the diphosphine ligands are shown to coordinate in a bridging fashion across the long, non-carbonyl-bridged Co(1)–Co(4) bond.

By way of contrast, the ORTEP diagram in Figure 3 shows that the unsaturated diphosphine dppt binds to the cluster IV in a chelating mode at a single Co center, as also deduced from the IR spectrum (vide supra).

The disubstituted clusters III and IV thus all belong to the general class consisting of four cobalt atoms in a rectangular array with the shorter sides bridged by μ-carbonyl groups.[20,22] The capping of the cobalt tetramer by a pair

(20) (a) The monosubstituted clusters with a dangling phosphine all displayed similar ν_{CO} bands in the IR [2056 (m), 2021 (vs), 2000 (s), and 1852 (m, br) cm^{-1} in CH_2Cl_2] to that of an independently prepared sample of $Co_4(CO)_9(PPh_3)(PPh_2)_2$. (b) Ryan, R. C.; Pittman, C. U.; O'Connor, J. P.; Dahl, L. F. *J. Organomet. Chem.* **1980**, *193*, 247.

(21) The $^{31}P\{^1H\}$ NMR spectra of these clusters in $CDCl_3$ showed three resonances at δ 135, 32, and –20 with a relative intensity of 2:1:1, respectively. These chemical shifts from low to high field are readily assigned to the μ_4-phosphinidene caps, coordinated phosphine, and dangling phosphine, respectively.
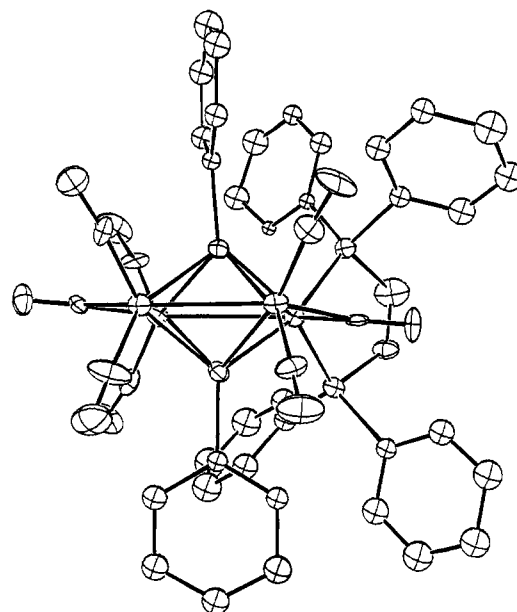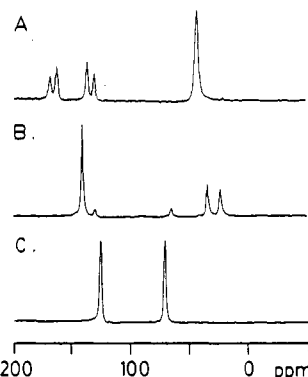
(22) Ryan, R. C.; Dahl, L. F. *J. Am. Chem. Soc.* **1975**, *97*, 6904.

Figure 5. The $^{13}C\{^1H\}$ NMR spectra of (A) $Co_4(CO)_8(PPh)_2$-(dppm) and (B) $Co_4(CO)_8(PPh)_2$(dppe) in 2-methyltetrahydrofuran solution at the temperatures indicated.

of μ_4-phenylphosphinidene groups completes the overall octahedral Co_4P_2 core common to this class. Selected bond lengths and bond angles in IIIa,b and IV are included in Tables I and II, respectively.

IV. Temperature-Dependent NMR Spectra of the Tetracobalt Clusters. The tetracobalt cluster I in dichloromethane solution at 25 °C showed a single, broad resonance at $\delta \sim 135$ due to the pair of phosphinidene caps in the proton-decoupled ^{31}P NMR spectrum.[23] The disubstituted derivatives III and IV also exhibited broad unresolved resonances for the capping phosphinidenes and the diphosphine ligand at 25 °C. However these resonances were clearly resolved upon cooling the dichloromethane solutions to 198 K, as shown in Figure 4.[24] In particular, the ^{31}P spectrum of $Co_4(CO)_8(PPh)_2$(dppm) (IIIa) in Figure 4a showed three sets of ^{31}P resonances in an integral ratio of 1:1:2 at δ 163, 131, and 43, respectively. The AB quartet at low field was readily assigned to the pair of phosphinidene caps—the resonance centered at 163 ppm being assigned to the μ_4-PPh cap that is located in the octahedral face above which the dppm ligand is located. The coupling constant of 218 Hz results from the splitting of the inequivalent phosphinidene caps.[27] The bridging dppm ligand was observed as a singlet at δ 43. Only quadrupolar broadening of all the ^{31}P resonances was
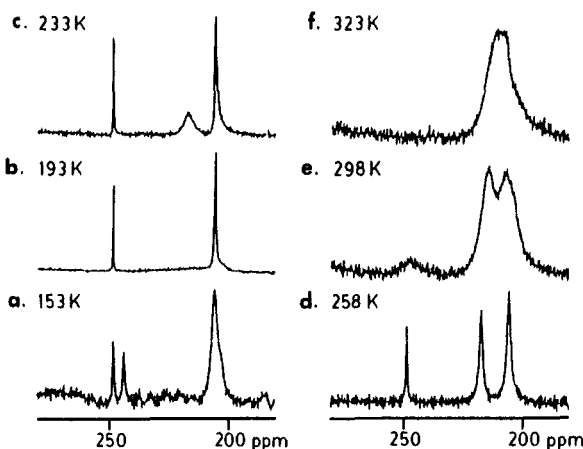

Figure 6. Temperature dependence of the $^{13}C\{^1H\}$ NMR spectrum of $Co_4(CO)_8(PPh)_2$(dppt) (IV) in 2-methyltetrahydrofuran solution at the temperatures indicated.

observed upon gradually warming the solutions.[25] The $^{31}P\{^1H\}$ NMR spectrum in Figure 4b of $Co_4(CO)_8(PPh)_2$-(dppe) (IIIb), whose solid-state structure was similar to that of the dppm analogue, showed three ^{31}P resonances in a 2:1:1 integral ratio with δ 130, 31, and 20, respectively.[29] The chemical shifts accorded with an assignment of the low-field singlet to the pair of μ_4-phosphinidene caps and the high-field pair of resonances to the dppe ligand. The latter resonances were observed to coalesce as the temperature was raised to 228 K with a weighted-average chemical shift of ~ 25 ppm. This temperature-dependent behavior which differs from that of IIIa was ascribed to a stereoequilibration of the pair of bonded Co centers as a result of a more flexible dppe bridge. Indeed the estimated[30] activation parameter $\Delta G^\ddagger \simeq 10$ kcal mol^{-1} accorded with those previously evaluated for the bridge-terminal carbonyl interchanges via a mutual exchange mechanism in the parent cluster and in its phosphite derivatives.[31] Finally, the $^{31}P\{^1H\}$ NMR spectrum in Figure 4c of $Co_4(CO)_8(PPh)_2$(dppt) (IV) showed two resonances at δ 125 and 77 in a 1:1 integral ratio for the phosphinidene caps and dppt ligand, respectively.

The dynamic behavior of the carbonyl ligands in the diphosphine derivatives III and IV was examined by the temperature dependence of the ^{13}C NMR spectra. The limiting ^{13}C NMR spectrum of the parent tetracobalt cluster I at 173 K showed two resonances at δ 238 and 204 with relative intensities of 1:4 which were readily assigned to the pair of bridging CO's and the eight equivalent terminal CO's, respectively, in idealized D_{2h} symmetry.[31] Figure 5a showed the limiting ^{13}C NMR spectrum of $Co_4(CO)_8(PPh)_2$(dppm) (IIIa) to consist of three resonances at δ 245, 209, and 205. By analogy with that of I, the low-field resonance was readily assigned to the pair of equivalent bridging CO's. The terminal CO's attached to the cobalt atoms bearing the dppm ligand were expected to appear downfield (209 ppm) relative to those on the unsubstituted cobalt atoms (205 ppm).[32] A closer in-

(23) Garrou, P. E. *Chem. Rev.* **1981**, *81*, 229.

(24) The improved signal-to-noise and sharpened ^{31}P resonances at the lower temperature may be attributed to the thermal decoupling of the quadrupolar ^{59}Co ($I = {}^7/_2$) nucleus.[25,26]

(25) For discussions and examples of the temperature dependence on quadrupolar broadening in NMR, see: (a) Brevard, C.; Granger, P. *Handbook of High Resolution Multinuclear NMR*, Wiley: New York, 1981. (b) Harris, R. K. *Nuclear Magnetic Resonance Spectroscopy*; Pitman Books: Toronto, 1983. (c) Mann, B. E.; Taylor, B. F. *^{13}C NMR Data for Organometallic Compounds*; Academic: New York, 1981. (d) Aime, S.; Milone, L. *Prog. Nucl. Magn. Reson. Spectrosc.* **1977**, *11*, 183. (e) Todd, L. J.; Wilkinson, J. R. *J. Organomet. Chem.* **1974**, *80*, C31. (f) Gragg, B. R.; Layton, W. J. Niedenzu, K. *J. Organomet. Chem.* **1977**, *132*, 29. (g) Aime, S.; Milone, L.; Valle, M. *Inorg. Chim. Acta* **1976**, *18*, 9. (h) Aime, S.; Milone, L.: Osella, D.; Poli, A. *Inorg. Chim. Acta* **1978**, *30*, 45. (i) Aime, S.; Milone, L.; Rossetti, R.; Stanghellini, P. L. *Inorg. Chim. Acta* **1977**, *25*, 103.

(26) Further proof of the importance of the "thermal decoupling" phenomenon in these clusters comes from the temperature-dependent $^{31}P\{^1H\}$ NMR spectra of $Co_4(CO)_{10}(PPh)_2$. The ^{31}P NMR resonance of the capping phosphinidenes are observed to sharpen considerably upon cooling. Richmond, M. G.; unpublished results.

(27) This assignment has been confirmed in the ^{31}P NMR spectrum of various carbene derivatives of the parent tetracobalt cluster.[28]

(28) Richmond, M. G.; Kochi, J. K. *Organometallics*, in press.

(29) The source of the impurity in the ^{31}P NMR spectrum of Co_4-$(CO)_8(PPh)_2$(dppe) may be the chelated dppe derivative. Such chelating and bridging isomers of dppe have been differentiated by ^{31}P NMR on the basis of the large nuclear deshielding observed in the chelated coordination mode. For example, see: (a) Grim, S. O.; Briggs, W. L.; Barth, R. C.; Tolman, C. A.; Jesson, J. P. *Inorg. Chem.* **1974**, *13*, 1095. (b) Churchill, M. R.; Lashewycz, R. A.; Shapley, J. R.; Richter, S. I. *Inorg. Chem.* **1980**, *19*, 1277. See also ref 28.

(30) We have assumed a simple two-site exchange and the equation used to calculate the free energy of activation is $\Delta G^\ddagger = 19.14 T_c(9.97 + \log T_c/\delta\nu)/0.239$.

(31) Richmond, M. G.; Kochi, J. K. *Inorg. Chem.* **1986**, *25*, 1334.

Table III. Temperature Dependence of the ^{13}C NMR Spectra of Tetracobalt Clusters II–IV[a]

tetracobalt cluster	carbonyl chemical shift[b]		T_c,[c] K	$\Delta G^{\ddagger}$,[d] kcal mol^{-1}
	terminal	bridge		
$Co_4(CO)_8(PPh)_2(dppm)$	209.4 (2), 205.1 (4)	244.8 (2)	323	13.7
$Co_4(CO)_8(PPh)_2(dppe)$	207.9 (2), 204.4 (4)	251.3 (1), 244.8 (1)	228	10.1
			323	13.7
$Co_4(CO)_8(PPh)_2(dppt)$	205.5 (6)	248.1 (1), 243.7 (1)	208	8.5
			323	13.5

[a] The ^{13}C NMR spectra were measured in 4:1 (v/v) mixture of 2-methyltetrahydrofuran and benzene-d_6 in the presence of 0.01 M Cr(acac)$_3$ at temperatures between 153 and 173 K. [b] Numbers in parentheses represent integral value of carbons. [c] Coalescence temperature. [d] See Experimental Section.

spection of Figure 5a showed the latter resonance to be broadened slightly in comparison to the other carbonyl resonances. When the solution is warmed, the carbonyl signals broadened more or less simultaneously and finally merged to a single broadened resonance at 323 K. The observed chemical shift of 210 ppm of the broadened signal was in good agreement with the weighted-average chemical shifts of the terminal and bridging carbonyls. The limiting ^{13}C NMR spectrum in Figure 5b of $Co_4(CO)_8(PPh)_2(dppe)$ (IIIb) was similar to that of IIIa, except for the appearance of the μ-bridging carbonyls as two distinct resonances at 173 K. The two sets of carbonyl resonances at δ 251, 245, 208, and 204 in a relative intensity ratio of 1:1:2:4 were readily assigned to a pair of bridging and terminal carbonyls, respectively. As the temperature was raised to 228 K, the pair of low-field resonances gradually broadened and merged into a broad resonance at 248 ppm. This low-energy exchange process with $\Delta G^{\ddagger} \simeq 10$ kcal mol^{-1} involved only the μ-carbonyl groups,[30] since the high-field pair of resonances were relatively unchanged. The similar temperature dependence of the coalescence of the ^{13}C and the ^{31}P NMR spectra suggested that a common process was operative which equilibrated both the dppe ligand as well as the bridging carbonyls. At this temperature the clusters IIIa and IIIb became spectroscopically similar. Further warming the solution of IIIb to 323 K afforded a single, broad resonance at 212 ppm which represented the weighted-average chemical shifts of all the terminal and bridging carbonyls. At this temperature the exchange of terminal and bridging carbonyls in IIIb was clearly similar to that in IIIa.

The limiting ^{13}C NMR spectrum in Figure 6a of $Co_4(CO)_8(PPh)_2(dppt)$ showed three carbonyl resonances at δ 248, 244, and 206 with a relative intensity ratio of 1:1:6 at 153 K. The resonance at lowest field (δ 248) was assigned to the bridging carbonyl attached to the disubstituted cobalt center (see Co(4) in Table I). The other bridging carbonyl was associated with the resonance at δ 244. At this low-temperature limit all the terminal carbonyls appeared as an unresolved singlet at 206 ppm. As the temperature was increased to 193 K in Figure 6b, the bridging carbonyl resonance at δ 248 remained essentially unchanged but that at δ 244 disappeared into the base line only to reappear at a higher temperature (Figure 6c at 233 K) as a broadened signal at 217 ppm, which was in agreement with the weighted-average chemical shifts of δ 244 and 206. This resonance continued to sharpen at 258 K in Figure 6d. As the temperature was raised to 298 K in Figure 6e, the remaining μ-carbonyl at δ 248 broadened.

At the high-temperature limit of 323 K in Figure 6f all the carbonyl resonances eventually coalesced into a single broadened resonance at ~216 ppm, which represented the weighted-average chemical shift of all the carbonyl resonances. The results in Table III summarize the dynamic ^{13}C NMR behavior of the disubstituted clusters IIIa,b and IV.

The temperature-dependent behavior of the ^{13}C NMR spectra of the tetracobalt clusters IIIa,b and IV was characteristic of the rapid exchange of bridge and terminal carbonyls via a mutual exchange mechanism[33] of the type involving a one-for-one, two-center process previously advocated by Lewis and co-workers for $Cp_2Rh_2(CO)_3$ and $Cp_2Rh_2(CO)_2[P(OPh)_3]$.[34,35]

Discussion

The tetracobalt cluster $Co_4(CO)_{10}(\mu_4\text{-}PPh)_2$ (I) reacts with a series of diphosphines II under thermal conditions at >80 °C or under ETC stimulation at 25 °C. The thermal reactions generally proceed inefficiently to afford disubstitution products in modest yields accompanied by material loss to interactable byproducts. By way of contrast, ETC catalysis with traces of benzophenone ketyl leads to good yields of both mono- and disubstitution products the relative amounts of which depend on the diphosphine structure. Thus the three- and four-membered diphosphines dppm, dppe, and dppt afford disubstitution products IIIa,b and IV, respectively, independent of whether thermal conditions or ETC catalysis is employed. The methods are however distinguished with the higher homologues of $Ph_2P(CH_2)_nPPh_2$. Thus the diphosphines dppp and dppb with $n = 3$ and 4 together with the chiral diop yield a rather complex mixture consisting mostly of disubstituted clusters when they are heated with I. These diphosphines under ETC catalysis afford high yields of pure monosubstituted cluster V that possesses a noncoordinated, dangling phosphine moiety, the structure of which is shown.

These divergent results can be accommodated in the light of our earlier studies of the tetracobalt cluster I with monophosphines.[31] Thus the activation barrier for ligand substitution of the tetracobalt cluster I under thermal conditions derives largely from an associative (S_N2-like) interaction.[36] On the other hand, Scheme I illustrates the

(32) (a) Cohen, M. A.; Kidd, D. R.; Brown, T. L. *J. Am. Chem. Soc.* 1975, *97*, 4408. (b) Todd, L. J.; Wilkinson, J. R. *J. Organomet. Chem.* 1974, *77*, 1. (c) Darensbourg, D. J.; Peterson, B. S.; Schmidt, R. E. *Organometallics* 1982, *1*, 306. (d) Johnson, B. F. G.; Lewis, J.; Reichert, B. E.; Schorpp, K. T. *J. Chem. Soc., Dalton Trans.* 1976, 1403. (e) Stuntz, G. F.; Shapley, J. R. *J. Am. Chem. Soc.* 1977, *99*, 607. (f) Darensbourg, D. J.; Zalewski, D. J.; Delord, T. *Organometallics* 1984, *3*, 1210. (g) Darensbourg, D. J.; Zalewski, D. J. *Organometallics* 1985, *4*, 92.

(33) For some reviews on fluxional processes in metal cluster compounds, see: (a) Band, E.; Muetterties, E. L. *Chem. Rev.* 1978, *78*, 639. (b) Johnson, B. F. G.; Benfield, R. E. In *Transition Metal Clusters*; Johnson, B. F. G., Ed.; Wiley: New York, 1980; Chapter 7. (c) Pregosin, P. S. *Annu. Rep. NMR Spectrosc.* 1981, *11a*, 227. (d) Cotton, F. A.; Hanson, B. E. In *Rearrangements in Ground and Excited States*; de Mayo, P., Ed.; Academic: New York, 1980; Vol. 2, Chapter 12.

(34) (a) Evans, J.; Johnson, B. F. G.; Lewis, J.; Norton, J. R. *J. Chem. Soc., Chem. Commun.* 1973, 79. (b) Evans, J.; Johnson, B. F. G.; Lewis, J.; Matheson, T. W. *J. Chem. Soc., Chem. Commun.* 1975, 576. (c) Evans, J.; Johnson, B. F. G.; Lewis, J.; Matheson, T. W.; Norton, J. R. *J. Chem. Soc., Dalton Trans.* 1978, 626.

(35) Cf. also the process described in ref 33a.

V
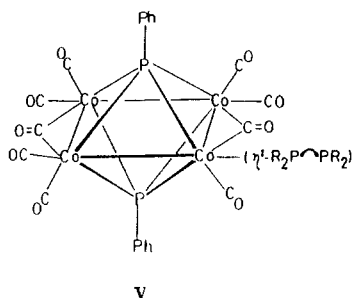
course of reaction under ETC catalysis in which CO loss from the labile anion radical $Co_4(CO)_{10}(PPh)_2^{\cdot-}$ is rate-limiting.[19] In such a process, the subsequent ring closure from the monosubstituted cluster V is facilitated by the shorter chain diphosphines such as the dppm and dppe.

As the phosphine separation increases in the higher homologues with $n = 3$ and 4, ETC catalysis leads to only monosubstitution despite the disubstitution that is obtained under thermal conditions. The latter undoubtedly reflects the higher activation energy associated with disubstitution that is compensated by a favorable entropic contribution in the lower homologues (vide supra).[37,38] The ring closure either by bridging the Co–Co bond or by chelating a single Co atom as in structures III and IV, respectively, is apparently balanced delicately since dppm or dppe with $n = 1$ and 2 favor the former whereas the more rigid dppt favors chelation.[39,41]

The dynamic behavior of such disubstituted clusters is provided by the temperature-dependent ^{13}C and ^{31}P NMR spectra. While the structures of $Co_4(CO)_8(PPh)_2(dppm)$ and $Co_4(CO)_8(PPh)_2(dppe)$ in the solid state (Figure 2) are similar, unique differences are observed in solution. For example, two distinct bridging carbonyls are revealed in the limiting ^{13}C NMR spectrum of the dppe cluster IIIb, whereas they are magnetically equivalent in the dppm analogue IIIa. The temperature-dependent behavior of the ^{13}C and ^{31}P NMR spectra of IIIb indicates the more or less simultaneous equilibration of the bridging carbonyls, and the dppe ligand occurs with an activation barrier

Scheme I

$\Delta G^{\ddagger} \simeq 10$ kcal mol^{-1}. The dynamic process consistent with the spectroscopic data is a rocking of the dppe ligand, as illustrated. Such a to-and-fro motion averages the dppe

cluster IIIb to essentially C_{2v} symmetry, as it is in the dppm analog IIIb (see Figure 2a). Indeed the similarity is underscored by the superposition of the cluster cores (Co_4) of IIIa and IIIb in the stereoscopic view presented in Figure 7. [Note that such an arbitrary operation leads automatically to the placement of the P(4) of the dppm and dppe ligands essentially on top of each other.]

The result clearly shows the skewing of the dppe ligand with respect to the more symmetrically bound dppm ligand. Furthermore the pertinent bond angles Co(1)–Co-(4)–P(4) and Co(4)–Co(1)–P(3) in $Co_4(CO)_8(PPh)_2(dppm)$ are 99° and 93°, respectively. The same angles are 100 and 111° in $Co_4(CO)_8(PPh)_2(dppm)$. Finally a higher energy process $(\Delta G^{\ddagger} \simeq 14$ kcal mol$^{-1})$ equilibrates the terminal as well as bridging carbonyls in IIIb in a manner similar to that observed in the dppm analogue IIIa.[42]

For the ethylenic analogue $Co_4(CO)_8(PPh)_2(dppt)$ (IV), the limiting ^{13}C NMR spectrum is consistent with X-ray structure in the solid state. The low-energy exchange of the bridging carbonyls shown in Figures 6a,b may be accounted for by the disposition of the diphosphine ligand dppt. Thus the chelation of dppt to a single cobalt atom leads to a lengthening of the Co(1)–Co(4) bond to 2.878 Å and a concomitant shortening of the Co(2)–Co(3) bond to 2.645 Å in comparison with average bond distances of ~ 2.70 Å in the dppm and dppe clusters IIIa and IIIb (see Table I). Furthermore the chelating phosphine in IV induces a twist about one of the μ_4-phosphinidene–phenyl bonds. Such structural alterations of the tetracobalt cluster are undoubtedly responsible for the facile carbonyl exchanges in $Co_4(CO)_8(PPh)_2(dppt)$.[43]

Experimental Section

Materials. The tetracobalt carbonyl $Co_4(CO)_{10}(\mu_4\text{-PPh})_2$ was prepared from sodium tetracarbonylcobaltate and dichlorophenylphosphine.[19] The diphosphines $(Ph_2P)_2CH_2$ (dppm), $(Ph_2P)_2(CH_2)_2$ (dppe), $(Ph_2P)_2(CH_2)_3$ (dppp), $(Ph_2P)_2(CH_2)_4$ (dppb), $Ph_2PCH=CHPPh_2$ (dppt), and $Ph_2PCH_2\overset{\frown}{C}(CH_3)OC$-

(36) (a) For similar kinetic behavior in other clusters, see: Karel, K. J.; Norton, J. R. *J. Am. Chem. Soc.* **1974**, *96*, 6813. Fox, J. R.; Gladfelter, W. L.; Geoffroy, G. L. *Inorg. Chem.* **1980**, *19*, 2574. Darensbourg, D. J.; Incorvia, M. J. *J. Organomet. Chem.* **1979**, *171*, 89. Darensbourg, D. J.; Incorvia, M. J. *Inorg. Chem.* **1980**, *19*, 2585. Stuntz, G. F.; Shapley, J. R. *J. Organomet. Chem.* **1981**, *213*, 389. Sonnenberger, D.; Atwood, J. O. *Inorg. Chem.* **1981**, *20*, 3243. Sonnenberger, D. C.; Atwood, J. D. *J. Am. Chem. Soc.* **1982**, *104*, 2113. Atwood, J. D.; Wovkulich, M. J.; Sonnenberger, D. C. *Acc. Chem. Res.* **1983**, *16*, 350. (b) The absence of a coordinatively unsaturated cluster of either $Co_4(CO)_9(\eta^1\text{-diphosphine})$-$(PPh)_2$ or the radical anion derived therefrom is as follows: (1) Carbon monoxide loss from species V in Scheme I has been found to be slow by ^{13}CO exchange studies. Richmond, M. G., unpublished results. (2) While dissociative loss of CO will occur from species A in Scheme I, it will do so only when all the starting cluster I has been consumed, thereby preventing the thermodynamically favored electron-transfer step.

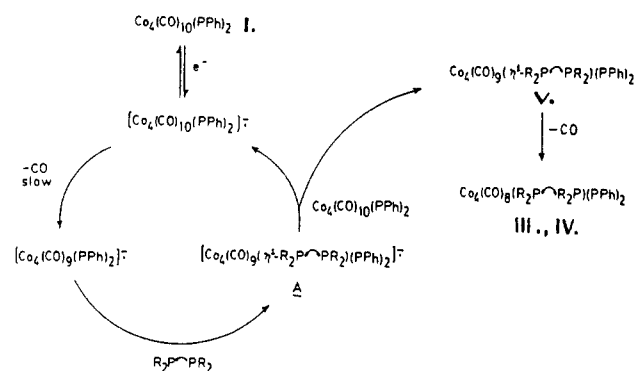(37) Basolo, F.; Pearson, R. G. *Mechanisms of Inorganic Reactions*; Wiley: New York, 1967.

(38) Such a ring closure is akin to neighboring group participation observed in many organic systems. For example, see: (a) March, J. *Advanced Organic Chemistry*; McGraw-Hill: New York, 1977. (b) Carey, F. A.; Sundberg, R. J. *Advanced Organic Chemistry*, Part A; Plenum: New York, 1977 and references within.

(39) There are other examples of chelating and bridge ring closure in inorganic complexes possessing η^1-bidentate ligands.[40]
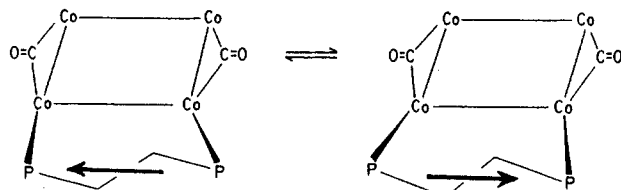
(40) (a) Plankey, B. J.; Rund, J. V. *Inorg. Chem.* **1979**, *18*, 957. (b) Poe, A.; Sekhar, V. C. *J. Am. Chem. Soc.* **1984**, *106*, 5034. (c) Mawby, R. J.; Morris, D.; Thorstein, E. M.; Basolo, F. *Inorg. Chem.* **1966**, *5*, 527. (d) Connor, J. A.; Day, J. P.; Jones, E. M.; McEwen, G. K. *J. Chem. Soc., Dalton Trans.* **1973**, *347*. (e) Kazlauskas, R. J.; Wrighton, M. S. *J. Am. Chem. Soc.* **1982**, *104*, 5784.

(41) See also (a) King, R. B.; Eggert, C. A. *Inorg. Chim. Acta* **1968**, *2*, 33. (b) King, R. B.; Kapoor, P. N. *Inorg. Chem.* **1969**, *8*, 1792. (c) King, R. B. *J. Coord. Chem.* **1971**, *1*, 67. (d) Cunninghame, R. G.; Doward, A. J.; Hanton, L. R.; Jensen, S. D.; Robinson, B. H.; Simpson, J. *Organometallics* **1984**, *3*, 180.

(42) For related examples, see ref 33–35.

(43) Clusters of this genre prefer to possess μ_4-phosphinidene phenyl groups which bisect the μ-bridging carbonyl groups and have similar bond lengths for the non-carbonyl-bridged Co–Co bonds. Deviations from such geometry lead to the general instability of the cluster as manifested by the solution and solid-state properties.
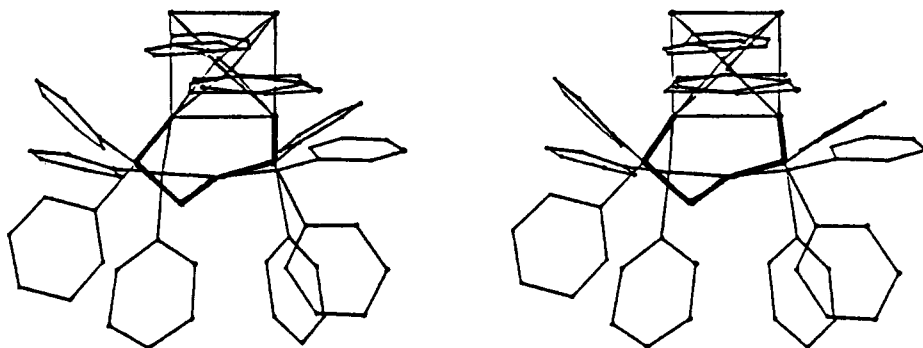
Figure 7. Stereoscopic view of the superposition of the Co_4 cores of the $Co_4(CO)_8(PPh)_2(dppm)$ and $Co_4(CO)_8(PPh)_2(dppe)$. The carbonyl groups are omitted for clarity.

Table IV. X-ray Crystallography Data for the Tetracobalt Clusters

	$Co_4(CO)_8(PPh)_2(dppm)^a$	$Co_4(CO)_8(PPh)_2(dppe)$	$Co_4(CO)_8(PPh)_2(dppt)$
space group	$P\bar{1}$, triclinic	$P\bar{1}$, triclinic	$P2_12_12_1$, orthorhombic
cell constants			
a, Å	10.735 (2)	11.732 (10)	10.982 (2)
b, Å	11.723 (2)	11.916 (8)	12.433 (1)
c, Å	12.674 (2)	19.116 (10)	32.832 (4)
α, deg	62.24 (1)	83.59 (5)	
β, deg	63.54 (1)	95.38 (6)	
γ, deg	64.86 (1)	120.41 (6)	
V, Å³	1215	2288.2	4483
mol formula	$C_{45}H_{32}Co_4P_4O_8{}^a$	$C_{46}H_{34}Co_4P_4O_8$	$C_{46}H_{32}Co_4P_4O_8$
fw	1102.9	1074.3	1072.4
formula units per cell (Z)	1	2	4
ρ, g cm⁻³	1.52	1.56	1.59
abs coeff (μ), cm⁻¹	15.7	16.1	16.44
radiatn Mo $K\alpha$ (λ), Å	0.710 73	0.710 73	0.710 73
collectn range	$4° \leq 2\theta \leq 40°$	$4° \leq 2\theta \leq 34°$	$4° \leq 2\theta \leq 40°$
scan width ($\Delta\theta$), deg	$0.90 + 0.35 \tan\theta$	$1.00 + 0.35 \tan\theta$	$0.90 + 0.35 \tan\theta$
max scan time, s	120	240	150
scan speed range, deg min⁻¹	0.7–5.0	0.30–3.35	0.6–5.0°
total data collected at 20 °C	2250	2662	2414
independent data, $I > 3\sigma(I)$	1952	1874	1438
$R = \sum\|\|F_o\| - \|F_c\|\|/\sum\|F_o\|$	0.044	0.064	0.044
$R_w = [\sum_w(\|F_o\| - \|F_c\|)^2/\sum w\|F_o\|^2]^{1/2}$	0.056	0.075	0.038
weights	$w = \sigma(F)^{-2}$	$w = \sigma(F)^{-2}$	$w = \sigma(F)^{-2}$

^{a} With $^1/_2$ CH_2Cl_2.

$(CH_3)_2OC(CH_3)CCH_2PPh_2$ ((+)-diop) were obtained from Strem Chemical and used as received. Toluene, benzene, and tetra-hydrofuran (THF) were reagent grade solvents that were redistilled from sodiobenzophenone under argon and stored in Schlenk flasks. Carbon monoxide (99% ^{13}C enriched) was obtained from the Mound Laboratory, Monsanto Research Corp.

Synthesis of $CO_4(CO)_8(PPh)_2(dppm)$ (IIIa). To 0.5 g (0.68 mmol) of $Co_4(CO)_{10}(PPh)_2$ and 0.29 g (0.71 mmol) of bis(diphenylphosphino)methane in 50 mL of THF was added 0.3 mL of a 0.025 M potassium benzophenone ketyl solution. The initial red color became red-brown immediately, and stirring was continued overnight at room temperature. TLC revealed the disubstituted cluster IIIa to be the major product. Isolation and purification were achieved by column chromatography on silica gel using a 1:1 mixture of benzene and hexane. An analytical sample and crystals suitable for X-ray crystallographic analysis were obtained by recrystallization from a 1:1 mixture of CH_2Cl_2 and hexane at -40 °C: yield 0.45 g (62.2%) of dark red crystals of $Co_4(CO)_8(PPh)_2(dppm)$; IR (CH_2Cl_2) ν_{CO} 2039 (vs), 1991 (vs), 1836 (m) cm⁻¹; $^{31}P\{^1H\}$ NMR (2-methyltetrahydrofuran/benzene-d_6, 4:1 (v/v); -75 °C) 163 (1 P, d, $J_{\mu_4-P-\mu_4-P}$ = 218 Hz), 131 (1 P, d, $J_{\mu_4-P-\mu_4-P}$ 218 Hz), 43 ppm (2 P, s). Anal. Calcd for $C_{45}H_{32}Co_4O_8P_4·CH_2Cl_2$: C, 48.26; H, 2.97. Found: C, 48.05; H, 3.07.

Synthesis of $Co_4(CO)_8(PPh)_2(dppe)$ (IIIb). To 0.2 g (0.27 mmol) of $Co_4(CO)_{10}(PPh)_2$ and 0.12 g (0.3 mmol) of 1,2-bis(diphenylphosphino)ethane in 35 mL of THF was added ~0.2 mL of a 0.025 M potassium benzophenone ketyl. The initial red color became red-brown immediately, and stirring was continued for 3.0 h at room temperature. TLC showed the major product to be the desired cluster IIIb, which was isolated and purified by

chromatography on Florisil using a 1:1 mixture of benzene and hexane. An analytical sample and crystals suitable for X-ray crystallographic analysis were obtained by recrystallization from a 1:4 mixture of CH_2Cl_2 and hexane at -20 °C: yield 0.13 g (44.0 %) of dark red $Co_4(CO)_8(PPh)_2(dppe)$; IR (CH_2Cl_2) ν_{CO} 2039 (vs), 2000 (sh), 1989 (vs), 1827 (m, br) cm⁻¹; $^{31}P\{^1H\}$ NMR (2-methyltetrahydrofuran/benzene-d_6, 4:1 (v/v); -75 °C) δ 138 (2 P, s), 31 (1 P, s), 20 (1 P, s). Anal. Calcd for $C_{46}H_{34}Co_4O_8P_4$: C, 51.42; H, 3.17. Found: C, 50.60; H, 3.34.

Synthesis of $Co_4(CO)_8(PPh)_2(dppt)$ (IV). To 0.52 g (0.71 mmol) of $Co_4(CO)_{10}(PPh)_2$ and 0.34 g (0.86 mmol) of cis-1,2-bis(diphenylphosphino)ethylene in 50 mL of THF was added 1.0 mL of a 0.025 M potassium benzophenone ketyl. The reaction was then stirred overnight at room temperature. TLC examination revealed the presence of a slower moving material, which was isolated and purified by column chromatography on silica gel using a 1:1 mixture of benzene and hexane. The analytical sample and crystals suitable for X-ray crystallographic analysis were obtained by recrystallization from a 1:20 mixture of CH_2Cl_2 and hexane at -40 °C: yield 0.48 g (63.1%) of red-black $Co_4(CO)_8(PPh)_2(dppt)$; IR (CH_2Cl_2) ν_{CO} 2041 (vs), 2008 (vs), 1988 (vs), 1849 (m), 1813 (m) cm⁻¹; $^{31}P\{^1H\}$ NMR (2-methyltetrahydrofuran/benzene-d_6, 4:1 (v/v); -75 °C) δ 125 (2 P, s), 71 ppm (2 P, s). Anal. Calcd for $C_{46}H_{32}Co_4O_8P_4$: C, 51.52; H, 2.99. Found: C, 51.44; H, 3.04.

Synthesis of $Co_4(CO)_9(PPh)_2(diphosphine)$ (V). The ETC reaction between $Co_4(CO)_{10}(PPh)_2$ and 1,3-bis(diphenylphosphino)propane is described in detail. The other longer chain bidentate phosphines reacted to afford the analogous products in similar yields. To 0.5 g (0.68 mmol) of $Co_4(CO)_{10}(PPh)_2$ and 0.34 g (0.82 mmol) of 1,3-bis(diphenylphosphino)propane in 50 mL of THF was added ~1.0 mL of 0.025 M potassium ben-

Table V. Final Positional Coordinates of the Tetracobalt Clusters IIIa,b and IV (Non-Hydrogen Atoms Only)[a]

atom	x	y	z	B, Å²	atom	x	y	z	B, Å²
			Co₄(CO)₈(PPh)₂(dppm)·¹/₂CH₂Cl₂ (IIIa)						
Co(1)	0.474	0.517	0.373	2.15 (5)	C(15)	0.233 (2)	1.019 (1)	0.022 (1)	5.1 (4)*
Co(2)	0.3009 (2)	0.5216 (2)	0.5879 (2)	2.55 (5)	C(16)	0.283 (1)	0.886 (1)	0.362 (1)	3.2 (3)*
Co(3)	0.5201 (2)	0.5105 (2)	0.6473 (1)	2.57 (5)	C(21)	0.570 (1)	0.207 (1)	0.608 (1)	2.5 (3)*
Co(4)	0.6987 (2)	0.5074 (2)	0.4321 (1)	2.18 (5)	C(22)	0.493 (2)	0.144 (1)	0.604 (1)	4.0 (3)*
Cl(1)	-0.024 (2)	-0.007 (1)	0.830 (1)	11.1 (4)*	C(23)	0.531 (2)	0.005 (1)	0.645 (1)	4.7 (4)*
Cl(2)	0.081 (1)	0.202 (1)	0.6133 (9)	7.6 (3)*	C(24)	0.647 (2)	-0.070 (1)	0.688 (1)	4.2 (4)*
P(1)	0.4620 (3)	0.6423 (3)	0.4699 (3)	2.19 (9)	C(25)	0.728 (2)	-0.012 (2)	0.694 (1)	5.3 (4)*
P(2)	0.5270 (4)	0.3878 (3)	0.5521 (3)	2.4 (1)	C(26)	0.687 (1)	0.188 (1)	0.650 (1)	3.5 (3)*
P(3)	0.5409 (3)	0.6605 (3)	0.1794 (3)	2.22 (9)	C(31)	0.651 (1)	0.575 (1)	0.067 (1)	2.6 (3)*
P(4)	0.7743 (3)	0.6668 (3)	0.2608 (3)	2.43 (9)	C(32)	0.775 (2)	0.470 (1)	0.085 (1)	4.4 (4)*
O(1)	0.173 (1)	0.553 (1)	0.4119 (9)	6.2 (4)	C(33)	0.858 (2)	0.395 (1)	0.007 (1)	4.8 (4)*
O(2)	0.8197 (9)	0.4914 (9)	0.5969 (8)	4.2 (3)	C(34)	0.819 (2)	0.433 (2)	-0.100 (1)	5.3 (4)*
O(3)	0.537 (1)	0.2995 (9)	0.2905 (9)	5.5 (3)	C(35)	0.700 (2)	0.534 (2)	-0.120 (2)	6.3 (5)*
O(4)	0.056 (1)	0.742 (1)	0.652 (1)	7.3 (5)	C(36)	0.616 (2)	0.607 (1)	-0.039 (1)	4.2 (3)*
O(5)	0.175 (1)	0.305 (1)	0.781 (1)	6.3 (4)	C(41)	0.411 (1)	0.796 (1)	0.102 (1)	2.2 (3)*
O(6)	0.405 (1)	0.7324 (8)	0.7416 (8)	5.3 (3)	O(42)	0.288 (1)	0.770 (1)	0.125 (1)	3.8 (3)*
O(7)	0.539 (1)	0.285 (1)	0.8743 (9)	6.6 (4)	C(43)	0.180 (2)	0.869 (1)	0.068 (1)	5.0 (4)*
O(8)	0.910 (1)	0.2791 (9)	0.3637 (9)	5.4 (4)	C(44)	0.201 (2)	0.993 (2)	-0.006 (1)	5.3 (4)*
C(1)	0.276 (1)	0.537 (1)	0.435 (1)	4.3 (5)	C(45)	0.322 (2)	1.023 (2)	-0.024 (1)	5.3 (4)*
C(2)	0.735 (1)	0.500 (1)	0.565 (1)	2.2 (3)	C(46)	0.429 (2)	0.920 (1)	0.026 (1)	4.4 (4)*
C(3)	0.518 (1)	0.384 (1)	0.324 (1)	3.4 (4)	C(51)	0.959 (1)	0.602 (1)	0.162 (1)	2.2 (3)*
C(4)	0.153 (2)	0.657 (2)	0.624 (1)	4.5 (5)	C(52)	1.061 (1)	0.531 (1)	0.222 (1)	3.3 (3)*
C(5)	0.224 (1)	0.390 (1)	0.699 (1)	4.0 (5)	C(53)	1.204 (2)	0.480 (1)	0.161 (1)	4.3 (4)*
C(6)	0.458 (1)	0.650 (1)	0.703 (1)	3.4 (4)	C(54)	1.242 (2)	0.504 (2)	0.034 (2)	5.9 (4)*
C(7)	0.530 (1)	0.374 (1)	0.784 (1)	3.4 (4)	C(55)	1.145 (2)	0.571 (2)	-0.023 (1)	6.5 (5)*
C(8)	0.827 (1)	0.366 (1)	0.393 (1)	2.9 (4)	C(56)	0.995 (1)	0.629 (1)	0.039 (1)	4.0 (3)*
C(9)	0.658 (1)	0.752 (1)	0.161 (1)	2.7 (4)	C(61)	0.798 (1)	0.810 (1)	0.270 (1)	3.1 (3)*
C(10)	0.104 (5)	0.028 (4)	0.680 (4)	9 (1)*	C(62)	0.849 (1)	0.788 (1)	0.362 (1)	3.9 (3)*
C(11)	0.394 (1)	0.824 (1)	0.418 (1)	2.4 (3)*	C(63)	0.372 (2)	0.891 (2)	0.367 (1)	5.2 (4)*
C(12)	0.458 (1)	0.900 (1)	0.426 (1)	3.4 (3)*	C(64)	0.842 (2)	1.014 (2)	0.288 (1)	5.6 (4)*
C(13)	0.399 (2)	1.044 (2)	0.381 (1)	5.5 (4)*	C(65)	0.790 (2)	1.044 (2)	0.193 (2)	5.9 (4)*
C(14)	0.289 (2)	1.094 (2)	0.332 (2)	6.0 (4)*	C(66)	0.772 (1)	0.940 (1)	0.182 (1)	4.0 (3)*
			Co₄(CO)₈(PPh)₂(dppe) (IIIb)						
Co(1)	0.5293 (2)	0.4411 (3)	0.2995 (2)	3.03 (9)	C(21)	0.266 (2)	0.465 (2)	0.214 (1)	3.0 (5)*
Co(2)	0.3099 (2)	0.2505 (3)	0.3375 (2)	3.60 (9)	C(22)	0.266 (2)	0.546 (2)	0.257 (1)	4.1 (6)*
Co(3)	0.2635 (2)	0.1627 (3)	0.2085 (2)	3.43 (9)	C(23)	0.215 (2)	0.626 (2)	0.244 (1)	4.1 (6)*
Co(4)	0.4833 (2)	0.3547 (3)	0.1702 (2)	3.15 (9)	C(24)	0.156 (2)	0.624 (2)	0.178 (1)	4.4 (6)*
P(1)	0.4564 (5)	0.2375 (5)	0.2756 (3)	3.2 (2)	C(25)	0.151 (2)	0.545 (2)	0.131 (1)	4.4 (6)*
P(2)	0.3398 (5)	0.3658 (5)	0.2336 (3)	3.2 (2)	C(26)	0.204 (2)	0.464 (2)	0.145 (1)	3.9 (6)*
P(3)	0.7346 (5)	0.4966 (6)	0.3409 (3)	3.5 (2)	C(31)	0.770 (2)	0.410 (2)	0.416 (1)	3.8 (6)*
P(4)	0.6843 (5)	0.3885 (5)	0.1512 (3)	3.3 (2)	C(32)	0.691 (2)	0.371 (2)	0.474 (1)	5.9 (7)*
O (1)	0.439 (1)	0.462 (2)	0.4309 (9)	7.2 (6)	C(33)	0.716 (2)	0.306 (2)	0.536 (1)	8.1 (8)*
O(2)	0.339 (1)	0.163 (1)	0.0658 (8)	6.8 (6)	C(34)	0.816 (2)	0.279 (2)	0.539 (1)	7.4 (8)*
O(3)	0.599 (1)	0.706 (1)	0.2546 (9)	6.2 (5)	C(35)	0.890 (2)	0.313 (2)	0.482 (1)	7.2 (8)*
O(4)	0.068 (1)	0.258 (2)	0.3560 (9)	8.8 (6)	C(36)	0.869 (2)	0.380 (2)	0.420 (1)	5.5 (6)*
O(5)	0.276 (1)	0.035 (1)	0.4420 (9)	8.4 (6)	C(41)	0.815 (2)	0.655 (2)	0.367 (1)	3.3 (5)*
O(6)	0.183 (1)	-0.111 (1)	0.2317 (9)	6.7 (6)	C(42)	0.783 (2)	0.685 (2)	0.428 (1)	5.8 (7)*
O(7)	0.002 (1)	0.119 (2)	0.155 (1)	9.3 (7)	C(43)	0.832 (2)	0.809 (2)	0.447 (1)	6.1 (7)*
O(8)	0.491 (1)	0.560 (1)	0.0693 (9)	8.6 (6)	C(44)	0.915 (2)	0.914 (2)	0.411 (1)	6.1 (7)*
C(1)	0.439 (2)	0.411 (2)	0.384 (1)	5.4 (8)	C(45)	0.948 (2)	0.890 (2)	0.350 (2)	8.2 (8)*
C(2)	0.369 (2)	0.216 (2)	0.118 (1)	5.2 (7)	C(46)	0.904 (2)	0.766 (2)	0.333 (1)	6.2 (7)*
C(3)	0.571 (2)	0.598 (2)	0.279 (1)	4.0 (6)	C(51)	0.789 (2)	0.546 (2)	0.105 (1)	2.7 (5)*
C(4)	0.162 (2)	0.258 (2)	0.350 (1)	4.7 (7)	C(52)	0.878 (2)	0.564 (2)	0.055 (1)	3.9 (6)*
C(5)	0.295 (2)	0.119 (2)	0.403 (1)	6.1 (8)	C(53)	0.956 (2)	0.683 (2)	0.024 (1)	4.8 (6)*
C(6)	0.221 (2)	0.002 (2)	0.219 (1)	2.6 (6)	C(54)	0.958 (2)	0.790 (2)	0.043 (1)	5.9 (7)*
C(7)	0.108 (2)	0.143 (2)	0.172 (1)	4.5 (8)	C(55)	0.871 (2)	0.777 (2)	0.091 (1)	5.7 (7)*
C(8)	0.489 (2)	0.482 (2)	0.106 (1)	5.9 (8)	C(56)	0.790 (2)	0.656 (2)	0.123 (1)	3.9 (6)*
C(9)	0.844 (2)	0.513 (2)	0.272 (1)	3.2 (6)	C(61)	0.692 (2)	0.277 (2)	0.099 (1)	3.4 (5)*
C(10)	0.797 (2)	0.396 (2)	0.229 (1)	4.0 (7)	C(62)	0.740 (2)	0.194 (2)	0.119 (1)	4.1 (6)*
C(11)	0.512 (2)	0.123 (2)	0.295 (1)	3.7 (5)*	C(63)	0.734 (2)	0.106 (2)	0.077 (1)	5.6 (7)*
C(12)	0.557 (2)	0.106 (2)	0.366 (1)	4.6 (6)*	C(64)	0.678 (2)	0.103 (2)	0.011 (1)	5.6 (7)*
C(13)	0.597 (2)	0.013 (2)	0.379 (1)	6.4 (7)*	C(65)	0.628 (2)	0.180 (2)	-0.015 (1)	5.7 (7)*
C(14)	0.598 (2)	-0.059 (2)	0.331 (1)	7.5 (8)*	C(66)	0.634 (2)	0.268 (2)	0.029 (1)	3.7 (5)*
C(15)	0.560 (2)	-0.042 (2)	0.264 (1)	5.9 (7)*					
C(16)	0.516 (2)	0.047 (2)	0.251 (1)	4.9 (6)*					
			Co₄(CO)₈(PPh)₂(dppt) (IV)						
Co(1)	0.2535 (2)	0.0833 (2)	0.30937 (7)	2.78 (6)	C(16)	0.030 (2)	-0.085 (1)	0.4197 (5)	2.8 (4)*
Co(2)	0.0340 (2)	0.1397 (2)	0.30609 (7)	2.82 (6)	C(17)	0.222 (1)	0.373 (1)	0.3122 (5)	2.2 (4)*
Co(3)	0.0372 (2)	0.2144 (2)	0.38150 (7)	2.81 (6)	C(18)	0.134 (1)	0.454 (1)	0.3098 (5)	3.1 (4)*
Co(4)	0.2575 (2)	0.1605 (2)	0.39200 (7)	2.47 (6)	C(19)	0.162 (2)	0.556 (2)	0.2969 (5)	4.2 (5)*
P(1)	0.1225 (5)	0.0582 (4)	0.3606 (1)	2.7 (1)	C(20)	0.282 (2)	0.573 (2)	0.2830 (5)	5.2 (6)*
P(2)	0.1836 (4)	0.2408 (2)	0.3352 (1)	2.2 (1)	C(21)	0.367 (2)	0.491 (2)	0.2833 (5)	4.0 (5)*
P(3)	0.3584 (5)	0.0452 (4)	0.4314 (2)	3.1 (1)	C(22)	0.336 (2)	0.391 (1)	0.2978 (5)	3.4 (5)*
P(4)	0.3983 (4)	0.2811 (5)	0.4088 (2)	3.0 (1)	C(23)	0.294 (2)	-0.012 (1)	0.4774 (5)	2.9 (5)*

Table V (Continued)

atom	x	y	z	B, Å²	atom	x	y	z	B, Å²
O(1)	0.134 (1)	0.060 (1)	0.2311 (3)	4.4 (3)	C(24)	0.275 (2)	-0.120 (2)	0.4838 (5)	4.8 (5)*
O(2)	0.131 (1)	0.240 (1)	0.4644 (3)	4.2 (3)	C(25)	0.221 (2)	-0.154 (2)	0.5186 (6)	6.1 (6)*
O(3)	0.324 (1)	-0.142 (1)	0.2945 (4)	7.1 (4)	C(26)	0.187 (2)	-0.086 (2)	0.5486 (6)	5.7 (6)*
O(4)	0.443 (1)	0.169 (1)	0.2553 (4)	8.1 (5)	C(27)	0.212 (2)	0.026 (2)	0.5424 (6)	5.5 (6)*
O(5)	-0.061 (1)	0.309 (1)	0.2528 (4)	5.4 (4)	C(28)	0.267 (2)	0.056 (1)	0.5071 (5)	4.5 (5)*
O(6)	-0.175 (1)	-0.005 (1)	0.3091 (4)	7.0 (4)	C(29)	0.440 (2)	-0.062 (2)	0.4066 (5)	3.8 (5)*
O(7)	-0.051 (1)	0.437 (1)	0.3937 (4)	6.6 (4)	C(30)	0.378 (2)	-0.155 (2)	0.3917 (5)	4.5 (5)*
O(8)	-0.184 (1)	0.120 (1)	0.4164 (4)	6.9 (4)	C(31)	0.443 (2)	-0.237 (2)	0.3710 (6)	6.6 (6)*
C(1)	0.135 (2)	0.084 (1)	0.2654 (5)	2.8 (5)	C(32)	0.560 (2)	-0.225 (2)	0.3652 (6)	7.5 (7)*
C(2)	0.143 (2)	0.214 (1)	0.4309 (5)	2.8 (5)	C(33)	0.628 (2)	-0.142 (2)	0.3795 (6)	7.1 (6)*
C(3)	0.298 (1)	-0.056 (2)	0.3034 (5)	3.8 (5)	C(34)	0.564 (2)	-0.061 (2)	0.4008 (5)	5.4 (6)*
C(4)	0.370 (2)	0.139 (1)	0.2792 (5)	3.5 (5)	C(35)	0.517 (1)	0.323 (1)	0.3719 (4)	1.9 (4)*
C(5)	-0.021 (1)	0.243 (1)	0.2755 (4)	3.1 (5)	C(36)	0.577 (1)	0.242 (1)	0.3514 (4)	1.5 (4)*
C(6)	-0.096 (2)	0.053 (1)	0.3072 (7)	6.2 (6)	C(37)	0.666 (2)	0.265 (2)	0.3206 (5)	4.9 (5)*
C(7)	-0.013 (1)	0.350 (1)	0.3872 (4)	4.3 (4)	C(38)	0.701 (2)	0.375 (2)	0.3193 (6)	5.5 (6)*
C(8)	-0.097 (2)	0.155 (1)	0.4035 (5)	4.1 (5)	(C39)	0.645 (2)	0.452 (2)	0.3400 (5)	2.9 (4)*
C(9)	0.477 (2)	0.119 (1)	0.4573 (5)	3.9 (5)	C(40)	0.554 (2)	0.429 (1)	0.3674 (5)	3.6 (5)*
C(10)	0.493 (1)	0.220 (2)	0.4485 (4)	6.0 (5)	C(41)	0.341 (2)	0.407 (1)	0.4316 (5)	3.0 (4)*
C(11)	0.060 (1)	-0.069 (1)	0.3784 (4)	2.4 (4)*	C(42)	0.281 (2)	0.478 (1)	0.4077 (5)	3.9 (5)*
C(12)	0.034 (2)	-0.155 (2)	0.3500 (5)	3.5 (4)*	C(43)	0.221 (1)	0.563 (1)	0.4268 (5)	3.6 (5)*
C(13)	-0.016 (2)	-0.250 (2)	0.3646 (5)	4.1 (5)*	C(44)	0.226 (2)	0.574 (2)	0.4693 (6)	6.4 (6)*
C(14)	-0.040 (2)	-0.261 (1)	0.4057 (5)	4.3 (5)*	C(45)	0.291 (2)	0.505 (2)	0.4921 (6)	5.4 (6)*
C(15)	-0.017 (2)	-0.183 (2)	0.4338 (5)	4.4 (5)*	C(46)	0.347 (2)	0.417 (2)	0.4725 (5)	4.9 (5)*

a Anisotropically refined atoms are given in the form of the isotropic equivalent thermal parameter defined as $(^4/_3)[a^2B(1,1) + b^2B(2,2) + c^2B(3,3) + ab(\cos \gamma) B(1,2) + ac(\cos \beta)B(1,3) + bc(\cos \alpha)B(2,3)]$. Asterisk identifies atom refined isotropically.

zephenone ketyl. The reaction mixture was stirred overnight at room temperature. TLC examination using a 7:3 mixture of benzene and hexane revealed a ~70% conversion to a slower moving material. IR and ^{31}P NMR analysis of the crude reaction mixture suggested the product to be $Co_4(CO)_9(\eta^1\text{-dppp})(PPh)_2$ (V). The product was isolated free of unreacted $Co_4(CO)_{10}(PPh)_2$ by chromatography on silica gel using a 7:3 mixture of benzene and hexane. An analytical sample was obtained by recrystallization from a 1:10 mixture of CH_2Cl_2 and hexane at -40 °C: yield 0.60 g (81.1%) of dark red $Co_4(CO)_9(PPh)_2(\eta^1\text{-dppp})$; IR (CH_2Cl_2) ν_{CO} 2056 (m), 2021 (vs), 1999 (vs), 1840 (m, br) cm^{-1}; ^{31}P$\{^1$H$\}$ NMR (CDCl$_3$, 25 °C) 134 (2 P, br s) 32 (1 P, br s), -20 ppm (1 P, d, J_{P-P} = 37 Hz). Anal. Calcd for $C_{48}H_{36}Co_4O_9P_4$: C, 51.63; H, 3.23. Found: C, 49.08; H, 4.08.

Synthesis of $Co_4(CO)_8(PPh)_2(dppp)$. The thermal reaction between $Co_4(CO)_{10}(PPh)_2$ and 1,3-bis(diphenylphosphino)propane is described in detail. The other longer chain bidentate phosphines reacted to afford low yields of the disubstituted cluster that were found to be a mixture of chelating and bridging isomers. Thus 0.1 g (0.14 mmol) of $Co_4(CO)_{10}(PPh)_2$ and 0.06 g (0.15 mmol) of 1,3-bis(diphenylphosphino)propane in 10 mL of toluene was heated at 70 °C for 6 h. TLC examination using a 1:1 mixture of hexane and benzene indicated the presence of a slower moving material (~10%). Most of the material remained at the origin. The slower moving component was isolated and purified by chromatography on silica gel using benzene as the eluant. The analytical sample was obtained by recrystallization from a 1:5 mixture of CH_2Cl_2 and hexane at -40 °C: yield 0.012 g (7.9%) of red-black $Co_4(CO)_8(PPh)_2(dppp)$; IR (hexane) ν_{CO} 2045 (s), 2016 (w), 2002 (vs), 1975 (m), 1865 (m), 1821 (w), 1790 (m) cm^{-1}; ^{31}P$\{^1$H$\}$ NMR (CDCl$_3$, 25 °C) δ 135 and 124 (2 P total, phosphinidene caps, bridging dppp complex at higher field), 31 and 23 (2 P total, dppp ligand, bridging dppp complex at higher field). Anal. Calcd for $C_{47}H_{36}Co_4O_8P_4$: C, 51.85; H, 3.31. Found: C, 51.60; H, 3.38.

Instrumentation. Infrared spectra were recorded on a Nicolet 10-DX FT spectrometer in either 0.1- or 1.0-mm NaCl cells. The ^{31}P (36.2-MHz) and ^{13}C (75.5-MHz) NMR spectra were recorded on JEOL FX-90Q and Nicolet 300 wide-bore spectrometers, respectively. The ^{31}P and ^{13}C NMR chemical shifts are referred to external 85% H_3PO_4 and tetramethylsilane, respectively. Positive chemical shifts are to low field of the external standard.

X-ray Diffraction Study of $Co_4(CO)_8(PPh)_2(dppm)\cdot ^1/_2CH_2Cl_2$. A large blackish purple tabular block of dimensions 0.60 × 0.40 × 0.30 mm was mounted on a glass fiber in a random orientation on an Enraf-Nonius CAD-4 automatic diffractometer. The radiation used was Mo Kα monochromatized by a dense graphite crystal assumed for all purposes to be 50% imperfect.

Final cell constants, as well as other information pertinent to data collection and refinement, are listed in Table IV. The Laue symmetry was determined to be 1, and from the systematic absences noted the space group was shown to be either $P1$ or $P\bar{1}$. Intensities were measured by using the θ–2θ scan technique, with the scan rate depending on the net count obtained in rapid prescans of each reflection. Two standard reflections were monitored periodically during the course of the data collection as a check of crystal stability and electronic reliability, and these showed no significant variation. In reducing the data, Lorentz and polarization factors were applied; however, no correction for absorption was made due to the small absorption coefficient. On the basis of an experimental density measurement and observed statistics of the unitary structure factors, the space group was determined to be the noncentrosymmetric $P1$. Thus one of the Co atoms was fixed at a location near the center of the unit cell, and the other three were quickly found by analysis of the Patterson map. The remaining non-hydrogen atoms were found in subsequent difference Fourier syntheses. Additionally, there was a partial methylene chloride solvent molecule of crystallization that was refined with a 50% population factor. The usual sequence of isotropic and anisotropic refinement was followed, after which all hydrogens were entered in ideally calculated positions. Hydrogen isotropic temperature factors were estimated on the basis of the thermal motion of the associated carbons. After all shift/esd ratios were less than 0.3, convergence was reached at the agreement factors listed in Table IV. No unusually high correlations were noted between any of the variables in the last cycle of least-squares refinement, and the final difference density map showed a maximum peak of about 1.2 e Å^{-3}, located near the Cl atoms. Refinement of the enantiomorphic set of atomic coordinates yielded a somewhat higher R value, and thus the reported structure is assumed to represent the correct absolute configuration. All calculations were made by using Molecular Structure Corp.'s TEXRAY 230 modifications of the SDP-PLUS series of programs. The fractional positional parameters for the non-hydrogen atoms of $Co_4(CO)_8(PPh)_2(dppm)\cdot ^1/_2CH_2Cl_2$ are included in Table V.

In $Co_4(CO)_8(PPh)_2(dppm)$, the dppm ligand is found to bridge adjacent cobalt centers via the long non-carbonyl-bridged cobalt–cobalt bond. The two carbonyl-bridged Co–Co bonds of 2.530 Å (average are 0.16 Å shorter than the non-carbonyl Co–Co bonds of 2.692 Å (average). The terminal Co–CO distances range from 1.738 (13) to 1.827 (15) Å with a mean of 1.771 Å. The longer bridging Co–CO distances show the asymmetric coordination that accompanies dppm substitution. Here the distances vary from 1.855 (15) to 2.040 (12) Å. Figure 8A shows the asymmetric bridging carbonyls in $Co_4(CO)_8(PPh)_2(dppm)$ via a cross section
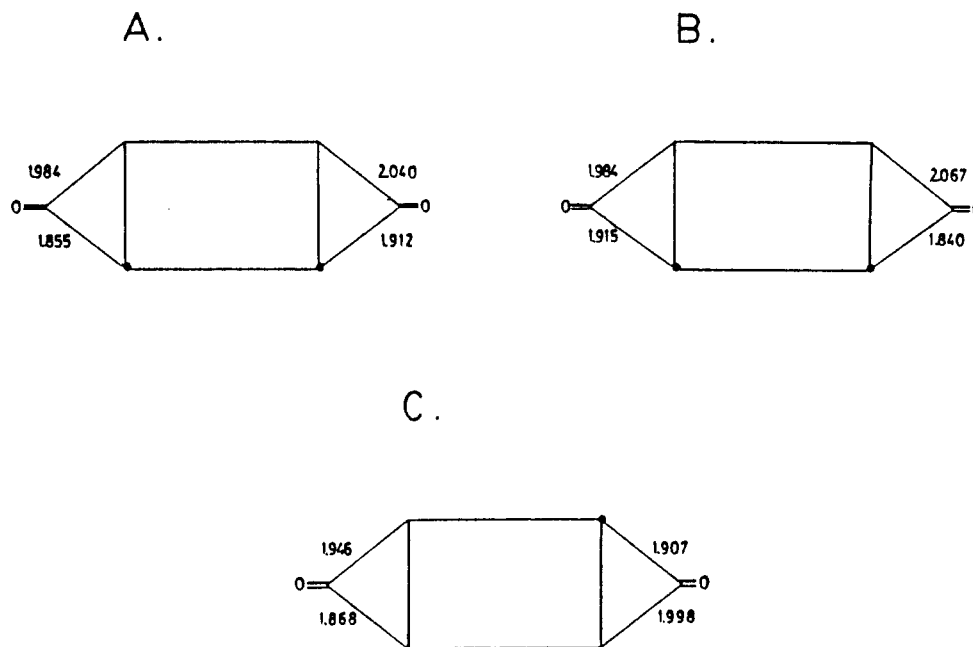
A.

1.984   2.040
O⚌   ⚌O
1.855   1.912

B.

1.984   2.067
O⚌   ⚌O
1.915   1.840

C.

1.946   1.907
O⚌   ⚌O
1.868   1.998

Figure 8. Comparison of the bridging Co–CO bond lengths (Å) in (A) $Co_4(CO)_8(PPh)_2(dppm)$, (B) $Co_4(CO)_8(PPh)_2(dppe)$, and (C) $Co_4(CO)_8(PPh)_2(dppt)$ as shown as the projection across the tetracobalt plane. The closed circles indicate cobalt atom substituted by at least one phosphine ligand.

through the tetracobalt plane. Similar observations regarding the shortening of the bridging OC–Co bond at a substituted cobalt center have also been noted by others.[20b,31] This may be ascribed to an electronic effect derived from ligand substitution by a phosphorus-centered nucleophile. The better σ-donating ability of the dppm ligand will place greater electron density on the cobalt at the site of substitution relative to that of an unsubstituted site. This manifests itself in a greater degree of π^*-back-bonding and diminution of the length of the bridging OC–Co bond at the site of substitution. The lengths of the Co–μ_4-P bonds of 2.243 Å (average) are in agreement with the bond lengths observed in the parent cluster $Co_4(CO)_{10}(PPh)_2$[20b,22] and support the absence of dppm ligand perturbation of the cluster framework. This conclusion is further reinforced by the essentially planar tetracobalt core and near parallel phosphinidene phenyl groups (twist angle 6.5°).[44]

X-ray Diffraction Study of $Co_4(CO)_8(PPh)_2(dppe)$. A small, deep red parallelepiped of approximate dimensions 0.30 × 0.30 × 0.25 mm was mounted on an Enraf-Nonius CAD-4 automatic diffractometer and otherwise located as described above. In reducing the data, Lorentz and polarization factors were applied, as well as an empirical absorption correction based on azimuthal ψ scans of six reflections having χ near 90°.[45] The structure was solved by use of MULTAN,[46] which revealed the positions of the eight cobalt and phosphorous atoms in the asymmetric unit. The usual sequence of isotropic and anisotropic refinement was followed, after which all hydrogens were entered in ideally calculated positions and held fixed. After all shift/esd ratios were less than 0.1, the full-matrix least squares converged at the agreement factors listed in Table IV. Anomalous dispersion coefficients for the heavier elements were included. No unusually high correlations were noted between any of the variables in the last cycle of least-squares refinement, and the final difference density map was featureless. All calculations were made as described above.

The disubstituted $Co_4(CO)_8(PPh)_2(dppe)$ (IIIb), like its dppm analogue, displays the bidentate phosphine ligand in a bridging fashion. The two carbonyl-bridged Co–Co bond lengths of 2.530

Å (average) and the nonbridged Co–Co bond lengths of 2.688 Å (average) are virtually identical with those in the dppm cluster IIIa and the parent cluster $Co_4(CO)_{10}(PPh)_2$.[20b,22] The terminal Co–CO distances vary from 1.693 (11) to 1.837 (12) Å with a mean distance of 1.781 Å (average). The bridging carbonyls are asymmetrically bound to the cluster with the shorter OC–Co bond distances being found at the cobalt center bearing the dppe ligand. The OC–Co distances range from 1.840 (12) to 2.067 (11) Å. Figure 8B shows bridging carbonyl cobalt bond distances via a cross section through the tetracobalt plane. The Co–μ_4-P distances of 2.243 Å (average), planar tetracobalt core, and near parallel phosphinidene phenyl groups (twist angle 8.6°) all suggest that the ancillary dppe ligand exerts no pronounced steric perturbation on the cluster framework.

X-ray Diffraction Study of $Co_4(CO)_8(PPh)_2(dppt)$. A very small black plate of approximate dimensions 0.30 × 0.25 × 0.07 mm was mounted on a glass fiber in a random orientation on an Enraf-Nonius CAD-4 automatic diffractometer and treated as described above. The Laue symmetry was determined to be *mmm* and from the systematic absences noted the space group was shown unambiguously to be $P2_12_12_1$. Intensities were measured by using the θ–2θ scan technique, with the scan rate depending on the net count obtained in rapid prescans of each reflection. Two standard reflections were monitored periodically during the course of the data collection as a check of crystal stability and electronic reliability, and these did not vary significantly. In reducing the date, Lorentz and polarization factors were applied; however, no correction for absorption was made. The structure was solved by MULTAN,[46] which revealed the positions of the four Co and four P atoms in the molecule. The remaining non-hydrogen atoms were found in subsequent difference Fourier syntheses. The usual sequence of isotropic and anisotropic refinement was followed, after which all hydrogens were entered in ideally calculated positions. Since there were so few observed data, the phenyl carbons had to be refined isotropically. Hydrogen temperature factors were estimated on the basis of the thermal motion of the associated carbons. The correct absolute configuration was determined by comparing the R values of the separate refinements of the two possible enantiomorphs $[R/R_w$ (+++) = 4.4/3.8% vs. (– – –) = 4.8/4.1%]. After all shift/esd ratios were less than 0.1, convergence was reached at the agreement factors listed in Table IV. No unusually high correlations were noted between any of the variables in the last cycle of least-squares refinement, and the final difference density map showed no peaks greater than 0.20 e Å^{-3}. All calculations were performed as described above.

(44) Extenuating cluster–ligand interactions usually lead to puckering in the tetracobalt plane and gross bond distance alteration in the non-carbonyl-bridged Co–Co bonds and Co–μ_4-P bonds. For example, see: (a) ref 20b. (b) Richmond, M. G.; Kochi, J. K. *Inorg. Chem.*, in press.

(45) North, A. C. T.; Phillips, D. C.; Matthews, F. S. *Acta Crystallogr., Sect. A: Cryst. Phys. Diffr., Theor. Gen. Crystallogr.* **1968**, *A24*, 351.

(46) Germain, G.; Main, P.; Woolfson, M. M. *Acta Crystallogr., Sect. A: Cryst. Phys., Diffr., Theor. Gen. Crystallogr.* **1971**, *A27*, 368.

$Co_4(CO)_8(PPh)_2(dppt)$ is the first structurally characterized example of a disubstituted cluster of this genre that possesses a chelating phosphine ligand. The chelating dppt ligand destabilizes the cluster core as evidenced by the alteration in the non-carbonyl-bridged Co–Co bonds. The non-carbonyl-bridged Co–Co bond adjacent to the chelating phosphine is 2.878 (3) Å while the other non-carbonyl-bridged Co–Co bond is 2.645 (3) Å. These lengths are 0.18 Å longer and 0.05 Å shorter, respectively, than the non-carbonyl-bridged Co–Co bond of 2.698 Å (average) observed in the parent cluster $Co_4(CO)_{10}(PPh)_2$.[22] This long non-carbonyl-bridged Co–Co bond length of 2.878 Å in cluster IV is the longest distance reported for this class of phosphinidene clusters. The carbonyl-bridged Co–Co bond lengths are similar, displaying a mean length of 2.524 Å (average). The carbonyl-bridged Co–Co bond lengths in IV are identical with those found in other structurally similar clusters.[20b,22,31] The terminal Co–CO lengths vary from 1.76 (2) to 1.81 (2) Å with a mean of 1.78 Å. The bridging Co–CO distances range from 1.907 (15) to 1.998 (14) Å (see Figure 8C). As previously noted, the Co–CO distance at the site of phosphine substitution is shorter than at the unsubstituted cobalt site. While the two bridging carbonyl OC–Co distances at both Co(1) and Co(2) are slightly different, their mean average distance 1.907 Å (average) is in agreement with the same distances in the parent cluster.[22] The lengths of the Co–μ_4-P bonds vary from 2.208 (4) to 2.280 (4) Å with an average distance of 2.254 Å, and the capping phosphinidene is found to be symmetrically bound to the tetracobalt core. The effect of the chelating phosphine on the perturbation of the ancillary ligands associated with the cluster is readily seen in the disposition of the phosphinidene phenyl groups. The plane formed by the phenyl group bound to P(1) and the tetracobalt plane possesses a dihedral angle of 83.6°. This represents a tipping of 6.4° away from the normally observed near perpendicular relation of these planes.[22,31] This phosphinidene phenyl group is tipped, presumably to avoid unfavorable interactions with the phenyl groups bound to P(3) of the chelating phosphine. The other phenyl group bound to P(2) undergoes a twist away from the preferred bisection of the bridging carbonyl Co–Co bonds. The twist angle between the two phosphinidene phenyl groups is ~73°. Finally, the twisting and tipping of these phosphinidene phenyl groups are necessary to avoid any close intramolecular contacts that would result with parallel phosphinidene phenyl groups and the chelating phosphine moiety. Furthermore, the lengthening of the non-carbonyl-bridged Co-(1)–Co(4) bond is believed to result from considerations similar to those discussed above.

Isotopic Enrichment of Tetracobalt Clusters IIIa,b and IV. ^{13}CO Enrichment of $Co_4(CO)_8(PPh)_2(dppm)$. To 0.1 g (0.09 mmol) of $Co_4(CO)_8(PPh)_2(dppm)$ (IIIa) in 10 mL of toluene was added ^{13}CO (1 atm). The reaction mixture was stirred at room temperature for 72 h and examined by IR, which indicated that essentially no enrichment had occurred. This suggests that intermolecular exchange of carbon monoxide is slow. The sample was then irradiated with 355-nm wavelength light (Rayonet Photochemical Reactor) for approximately 1 week at room temperature. The cluster was then recovered in essentially quantitative yield after purification by chromatography. The IR spectrum indicated the resulting product to be ~20% ^{13}CO enriched. The procedure described above was also used with clusters IIIb and IV with similar results.

Activation Energies from Temperature-Dependent ^{13}C NMR Spectra. The energies of activation in Table III were calculated according to the procedure given by Shanan-Atidi and Bar-Eli.[47,48] In this treatment the bridging carbonyls and terminal carbonyls were considered to be unequal doublets capable of undergoing intramolecular exchange. The relative populations of the carbonyls were obtained from the integration of the low-temperature (slow-exchange) spectrum. The variable-temperature ^{13}C NMR study allowed the determination of T_c, the coalescence temperature. At this temperature the observed chemical shift was found to be in good agreement with the weighted-average chemical shifts obtained from the slow-exchange spectrum. We have assumed that this behavior represents intramolecular carbonyl scrambling about the cluster polyhedron in all cases studied with the exception of the dppe rocking pathway which involves no carbonyl scrambling. Through the use of the relative populations of exchanging carbonyls and the coalescence temperature, the activation energy for intramolecular carbonyl scrambling was calculated with the aid of the modified Eyring equation.[49]

(47) Shanan-Atidi, H.; Bar-Eli, K. H. *J. Phys. Chem.* **1970**, *74*, 961.
(48) For a general review on dynamic processes and methods used to calculate activation energies, see: Sandstrom, J. *Dynamic NMR Spectroscopy*; Academic: New York, 1982.
(49) Glasstone, S.; Laidler, K. J.; Eyring, H. *The Theory of Rate Processes*, McGraw-Hill: New York, 1941.